# 3D Tumor Segmentation in MR images using Tumor Characteristics

**Arash Saeed Askari**

Submitted to the
Institute of Graduate Studies and Research
in partial fulfillment of the requirements for the degree of

Master of Science
in
Electrical and Electronic Engineering

Eastern Mediterranean University
August 2015
Gazimağusa, North Cyprus

Approval of the Institute of Graduate Studies and Research

Prof. Dr. Serhan Çiftçioğlu
Acting Director

I certify that this thesis satisfies the requirements as a thesis for the degree of Master of Science in Electrical and Electronic Engineering.

Prof. Dr. Hasan Demirel
Chair, Department of Electrical
and Electronic Engineering

We certify that we have read this thesis and that in our opinion it is fully adequate in scope and quality as a thesis for the degree of Master of Science in Electrical and Electronic Engineering.

Prof. Dr. Hasan Demirel
Supervisor

Examining Committee

1. Prof. Dr. Hasan Demirel
2. Asst. Prof. Dr. Hasan Abou Rajab
3. Asst. Prof. Dr. Rasime Uyguroğlu

# ABSTRACT

3D segmentation is an important pre-processing phase that dictates the performance of the possible post processing applications in 3D biomedical image analysis. 3D reconstruction of the segmented tumor from 2D MRI plays an essential role in 3D encapsulation of the segmented tumor. Fuzzy C-mean clustering is widely used in 2D segmentation of the brain tumor. In this thesis 2D tumor projections in each slice of the MRI are segmented using FCM. 2D slices extracted through FCM are used to generate the 3D reconstruction of the tumor. However, the possible low number of slices limits the quality of such 3D reconstruction. This thesis proposes to minimize this problem by generating predicted slices (P) between intra slices (I) and generating bi-predictive slices (B) between predictive slices and intra slices by using bilinear interpolation. 3D reconstruction of the brain tumor is performed by using the real slices and the predicted slices. Limitations of the FCM clustering in deciding which cluster is to be segmented is overcome by employing 2D/3D characteristics such as intensity, circularity and 3D Compactness in T2 -weighted MR Images for reliable segmentation of the 3D brain tumors. The proposed approach leads to detect the 3D tumor automatically with improved accuracy compared to alternative methods in the literature.

**Keywords:** 3D Segmentation; MRI; FCM clustering; Labeling; Thresholding; 3D reconstruction; 3D compactness; Circularity; Tumor; Brain.

# ÖZ

3D segmentasyon 3D Biyomedikal görüntü analizi gerektiren uygulamalarında performansı belirleyen önemli önemli bir ön-işleme aşamasıdır. 2D MRI kesimli tümörün 3D yeniden yapılanması, kesimli tümörün 3D kuşatılmasında önemli bir rol oynamaktadır. FCM kümeleme beyin tümörünün 2D düzlemde ayrılmasında yaygın olarak kullanılmaktadır. Bu tezde 2D tümör projeksiyonlarının MR görüntülemedeki her dilimi, FCM kullanılarak bölümlenmiştir. 2D dilimleri FCM içinden çıkarılan tümör 3D uzayında yeniden oluşturmak için kullanılmaktadır. Ancak, olası düşük dilim sayısı, 3D rekonstrüksiyon kalitesini sınırlamaktadır. Çift doğrusal enterpolasyon kullanarak gerçek dilimleri arasında öngörülen dilimler oluşturarak bu sorunu en aza indirmeyi öneriyoruz. Beyin tümörü 3D inşası gerçek dilimler ve tahmin edilen dilimler kullanarak gerçekleştirilir. FCM limitleri hangi kümenin ayrılması gerektigini belirleyemez. Beyin tümörlerinin güvenilir segmentasyonu için MR görüntüleri ağırlık, yoğunluk, dairesellik ve T2 3D kompaklık olarak 2D/3D özellikleri kullanılmaktadır. Önerilen yaklaşım literatürdeki alternatif yöntemler ile karşılaştırıldığında geliştirilmiş doğruluk ile 3D tümör otomatik olarak algılamaya yol açmaktadır.

**Anahtar kelimeler**: 3D segmentasyon; MRI; FCM kümeleme; Etiketleme; Eşikleme; 3D yeniden yapılanma; 3D anlatım; Döngüsellik; Tümör; Beyin

# DEDICATION

**To my lovely Wife and my Parents**

# ACKNOWLEDGMENT

First of all, I would like to thank my supervisor, Prof. Dr. Hasan Demirel, for his kindness, supervision, understanding, help and guidance throughout this study. His encouragement made me interested in image processing and 3D reconstruction.

Especially, I am deeply grateful to my beloved wife, Elham, for her endless love and Patience.

# TABLE OF CONTENTS

# LIST OF TABLES

# LIST OF FIGURES

# LIST OF SYMBOLS & ABBREVIATIONS

| | |
|---|---|
| $\varepsilon$ | Limitation principle |
| $\mu_i$ | Distance of k data from cluster centers |
| $\left\|x_i - \mu_j\right\|$ | Distance between object and cluster center |
| $\sigma$ | Sigma |
| $\omega$ | Line width |
| $\nabla^2 L$ | Laplacian operator |
| $\nabla$ | Derivative |
| A | Area |
| B | Bi-predictive slices |
| c | Number of Cluster |
| $d_{ij}$ | Euclidean distance measure |
| $C_U$ | High contrast |
| $C_L$ | Lower contrast |
| $C_r$ | Circularity Ratio |
| $C_R$ | Compactness ratio |
| D | Objective function for k-means |
| $H$ | Distance between two slices |
| I | Intra slices |
| $J_m$ | Objective function for FCM |
| k | Number of Cluster |
| $M_H$ | Average of gray value of H |
| $M_L$ | Average of gray value of L |
| p | Perimeter |

| | |
|---|---|
| P | Predictive Slices |
| $P_n$ | $n^{th}$ Partitions |
| $\mathbb{R}^2$ | 2D space |
| $\mathbb{R}^3$ | 3D space |
| $S_n$ | Area of the $n^{th}$ slice |
| T | Threshold |
| $T_0$ | Initial Threshold |
| T2w | Tissue value –weighted |
| $T_L$ | Lower threshold |
| $T_N$ | $n^{th}$ Threshold |
| $T_U$ | Upper threshold |
| $U^{(k)}, U^{(k+1)}$ | Optimal matrix norm |
| $V$ | Volume |
| $v_d$ | Volume between slices |
| $v_i$ | Center of the cluster |
| $x_i$ | Membership within $i^{th}$ cluster |
| $y_k$ | Membership within $i^{th}$ cluster |
| CCL | Connected component labeling |
| FCM | Fuzzy C-means |
| FP | False Positive |
| FN | False Negative |
| GTD | Ground truth data |
| MR | Magnetic Resonance |
| MRI | Magnetic Resonance Imaging |
| NMRI | Nuclear magnetic resonance imaging |

| | |
|---|---|
| NRI | Nuclear resonance imaging |
| PET | Positron Emission Tomography |
| ROI | Region of interest |
| TP | True Positive |
| TN | True Negative |

# Chapter 1

# INTRODUCTION

## 1.1 Introduction

Biomedical Image Analysis is the computer-based way of analyzing biomedical images using various methods. One of the pre-processing methodologies of image analysis is image segmentation which is defined to be the partitioning process of a digital images to the numerous groups of pixels which are regarded as segments. The primary reason for using image segmentation in medical images is to isolate the region of interest for further processing. The secondary reason is to create an alternative to the manual segmentation by experts which may be a laborious process that is time consuming.

Magnetic Resonance Imaging (MRI) is one of the techniques that is used to visualize the soft tissue of body. MR imaging technique is used in many cases to get high quality images of the soft tissues of the body. MRI is based on the axioms of nuclear magnetic resonance (NMR) which is a technique to obtain microscopic information about molecules. MRI was called magnetic resonance imaging instead of nuclear magnetic resonance imaging (NMRI) or nuclear resonance imaging (NRI) because of the negative connotations associated with the word nuclear in the late 1970's [1].

The Magnetic Resonance Imaging generates sequences of two dimensional 2D cross-sectional slices that have most of the 3D information of the studied organs which is

mostly used in medical imaging. Using those 2D slices helps to reconstruct the 3D volume and surface models of the tissues.

3D modeling of MR images are used in many medical applications. In the therapy period diagnosing the abnormalities is an important task. Moreover, detecting these abnormalities requires knowledge of characteristics [2], [3] and the location of the abnormality. Precise segmentation of brain tumor structure is a difficult process because it has lots of variety in shape, location and usually its intensity has overlap with the normal brain tissues.

This thesis proposes an automatic 3D segmentation and detection of brain tumor by utilizing Fuzzy C-means Clustering (FCM) [4], [5], for 2D segmentation and reconstruction from 2D tumor projections into a 3D tumor using slice interpolation and 3D surface rendering. 2D circularity measure is used to keep the tumor and filter out the non-tumor artifacts in the 2D slices. 3D compactness is used to keep the 3D tumors among the 3D reconstructed components. The results show that Accuracy, Specificity and Precision of the proposed 3D segmentation method are higher than K-mean clustering based approach as well as it is superior to similar methods in the literature.

## 1.2 Thesis Contributions

- 3D Tumor segmentation which contains Interpolation between 2D MR brain slices, Clustering of the 2D Slices and Tumor Extraction from Clustered Slices is studied.
- Interpolation between 2D MR slices is used as an optimization method to generate more slices.

- FCM is used as one of clustering algorithms to segment 2D MR slices.
- The superiority of the Fuzzy C-means based segmentation over K-means clustering is illustrated.
- Tumor Extraction based on 2D/3D characteristics of the tumor such as Tumor brightness, circularity and 3D compactness is analyzed.
- Circularity Ratio of the Thresholded slices is calculated.
- The performance of the proposed segmentation is compared with the k-means based method and some other existing methods by considering the performance analysis methods such as: Accuracy, Sensitivity, Precision, and Specificity.
- 3D Compactness of the Thresholded slices is calculated.
- 3D Compactness of the tumor based on FCM clustering and K-means clustering by using slice interpolation and without interpolation is computed.
- 3D reconstruction of the tumor by using 3D surface rendering is done.

## 1.3 Thesis overview

Chapter 1 as an introduction which reviews the Biomedical image Analysis, Magnetic Resonance Images and the problem explanation in manual MR images segmentation by expert, representing a solution by the outcome of applying the proposed method. In Chapter 2 general methods and applications for Brain Tumor segmentation in medical image processing is discussed. Furthermore, it deals with clustering topic and different methods in image clustering, K-means clustering and Fuzzy C-means clustering are two main standard methods which are introduced and explained mathematically. Chapter 3 contains a definition of feature extraction and 3D reconstruction of 2D MR slices and explained mathematically the surface rendering process which is used for 3D reconstruction of different components of the

medical images. Chapter 4 represent the proposed 3D brain tumor segmentation based of Fuzzy C-mean clustering and 3D characteristics of the tumor in detail with the block diagrams and images which show the whole process clearly. Experimental results and the comparison of them with the other methods which is shown in tables and graphs are in chapter 5. In the final chapter, chapter 6, the conclusion obtained by the proposed method is discussed and more effective method is recommended for a more accurate diagnosis of the brain tumor.

# Chapter 2

# IMAGE SEGMENTATION

## 2.1 Introduction

In Biomedical Image Processing, segmentation is an essential step in image analysis and the current techniques for recording and describing the image depends on the results of this phase. Segmentation aims to simplify or change the image to more meaningful and easier analysis.

The segmented area has a specific characteristic for instance, in satellite images forests, rivers or urban areas and in medical images an abnormality can be the region of interest (ROI) for segmentation. Segmentation is considered when the ROI does not cover the whole image. In that situation the ROI is called foreground area and the background area will be ignored. Choosing the ROI is very important. For example, the area which is selected for segmentation must be uniform and homogeneous with respect to intensity, color, texture and etc. Furthermore, it shouldn't have lots of holes in the interior area. Also it must be smooth and not ragged [5].

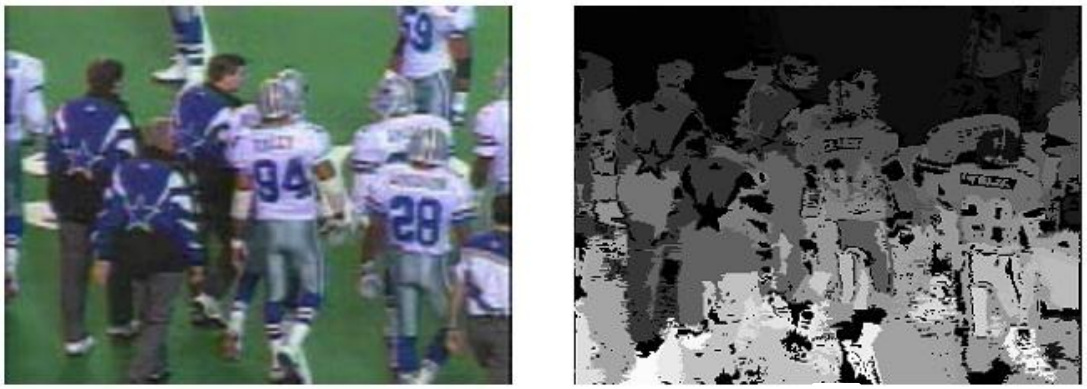

a b

Figure 2.1: a) Image of the football team, b) result after segmentation [5]

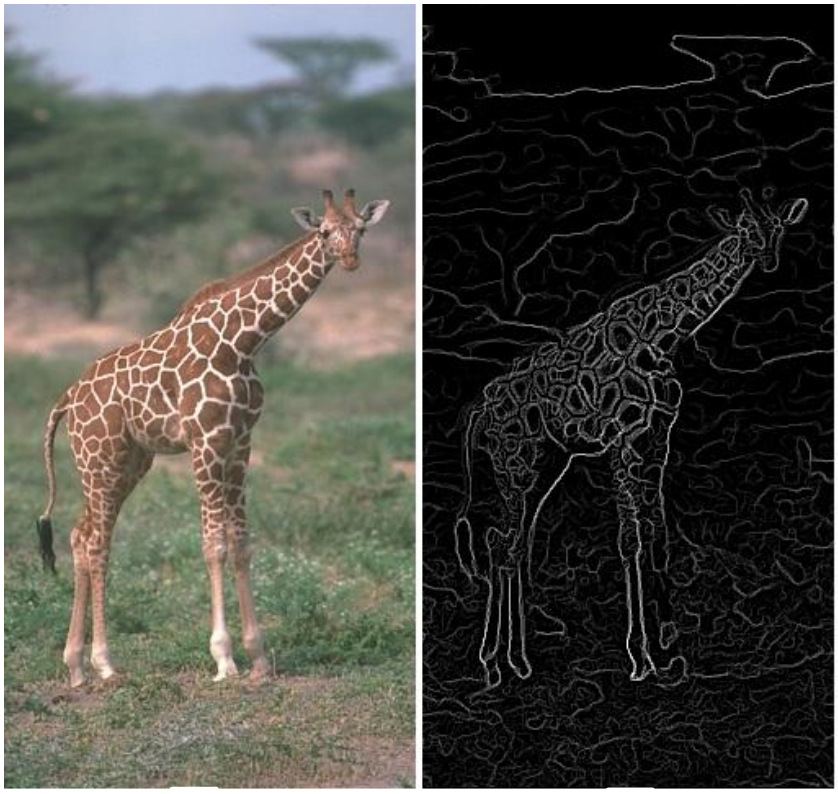

a b

Figure 2.2: a) Input image, b) Segmented Image by edge detection method [5]

The outcomes of the segmentation process may lead to Object Recognition, Image Compression and Image Editing. In another word, three main methods for image segmentation are as follows: Edge base Segmentation, Region base Segmentation and Pixel based Segmentation. These ways lead to several segmentation method such

as Thresholding methods, Histogram based methods, Region growing based method, Graph based methods, and Edge detection method, Clustering methods [4]. In this chapter some of the popular segmentation methods is illustrated.

## 2.2 Thresholding

Thresholding method is one of the utile methods that is used in image processing specially in medical images. Thresholding can convert the gray level image to multiple thresholds. By analyzing the image histogram we can classify the components of the image to multiple classes.

There are 6 groups that categorize the thresholding methods. Histogram shape-based methods. Clustering-based methods. Entropy-based methods. Cross-entropy between the original and binarized image, etc. Object attribute-based methods. The spatial methods. Local methods [6]

Thresholding create a binary image from a gray-level one. In this approach, the thresholding value must be chosen. This method convert the pixels which have the lower value with compare to thresholding value, to zero and the rest which are above that value to one.

If the image represented by *f(x, y)* with the thresholding value *T* the thresholded version of the image *g(x, y)* is obtained as follows:

$$g(x,y) = \begin{cases} 1 & if \quad f(x,y) > T \\ 0 & if \quad f(x,y) \le T \end{cases} \tag{2.1}$$

The binarized image has two classes, 1 and 0 which is obtained with respect to the thresholding value. To apply this method 5 step must be done.

1. Initial thresholding value must be defined ($T=T_0$).

2. In second step the gray-level divided in to two part, equal or less than $T_0$ and higher than $T_0$.
3. The average of the two obtained gray level values must be calculated. Assume that the value under the $T_0$ is L and the higher value is H. Thus $M_L$ and $M_H$ are the average values.
4. The new threshold is calculated as follows:

$$T_N = \frac{M_L + M_H}{2} \tag{2.2}$$

5. Until $T_N$ is less than $T_0$ step 2 and 4 must be recomputed.

Figure 2.3 shows a gray level image which is segmented by thresholding method. As you can see all the gray level values in image a converted to two binary values.

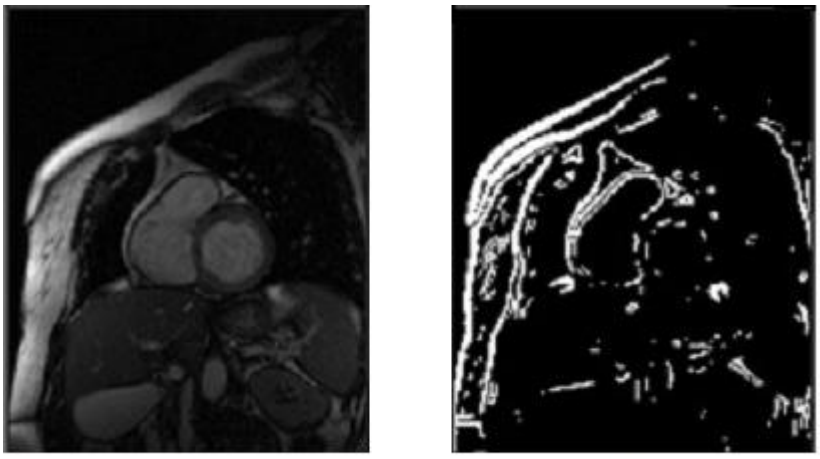

a b

Figure 2.3: a) Cardiac gray-level MRI, b) Segmented image using Thresholding [9]

## 2.3 Histogram based segmentation

Segmentation based on the Histogram of an image is one of the simplest and most useful methods in image segmentation. This method utilize the image histogram to classify the pixels into regions with respect to their gray-levels.

Two main parts of an image are Background and Foreground. Background is the most area in the image and in the histogram the large peak is related to its gray-level. The object in the image has different gray level and its peak in the histogram is smaller than Background. Figure 2. 4 illustrate the segmentation of the skin based on its Histogram.

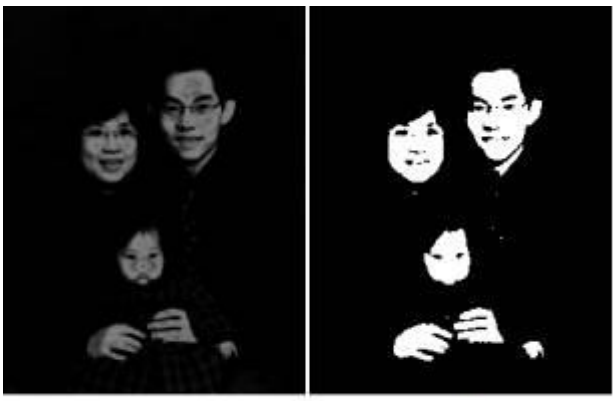

a b

Figure 2.4: a) gray-level image, b) Histogram based skin segmentation [61]

## 2.4 Image segmentation based on edge detection

The validation of many image processing techniques depends on the accuracy of detecting the meaningful edges in the image. Using gray tones changes in the image to transform that main image to edge image is a technique that is called Edge Detection. The results of this transform shows that there is no changes in physical quality between the prior and the edge image [10], [11]. Some main reasons such as

noise, segmentation errors, overlap, and variation of the intensity lead us to use edge detection technique [12].

There are three steps to detect the objects edges. First filtering, to remove the existing noises in the image [13]. Second enhancement and third detection. In addition there are 3 main methods for edge detection: 1- The Roberts Detection, 2- The Prewitt Detection and 3- The Sobel Detection. Figure 2.6 shows the results of these methods.


Figure 2.5: Original image before edge detection

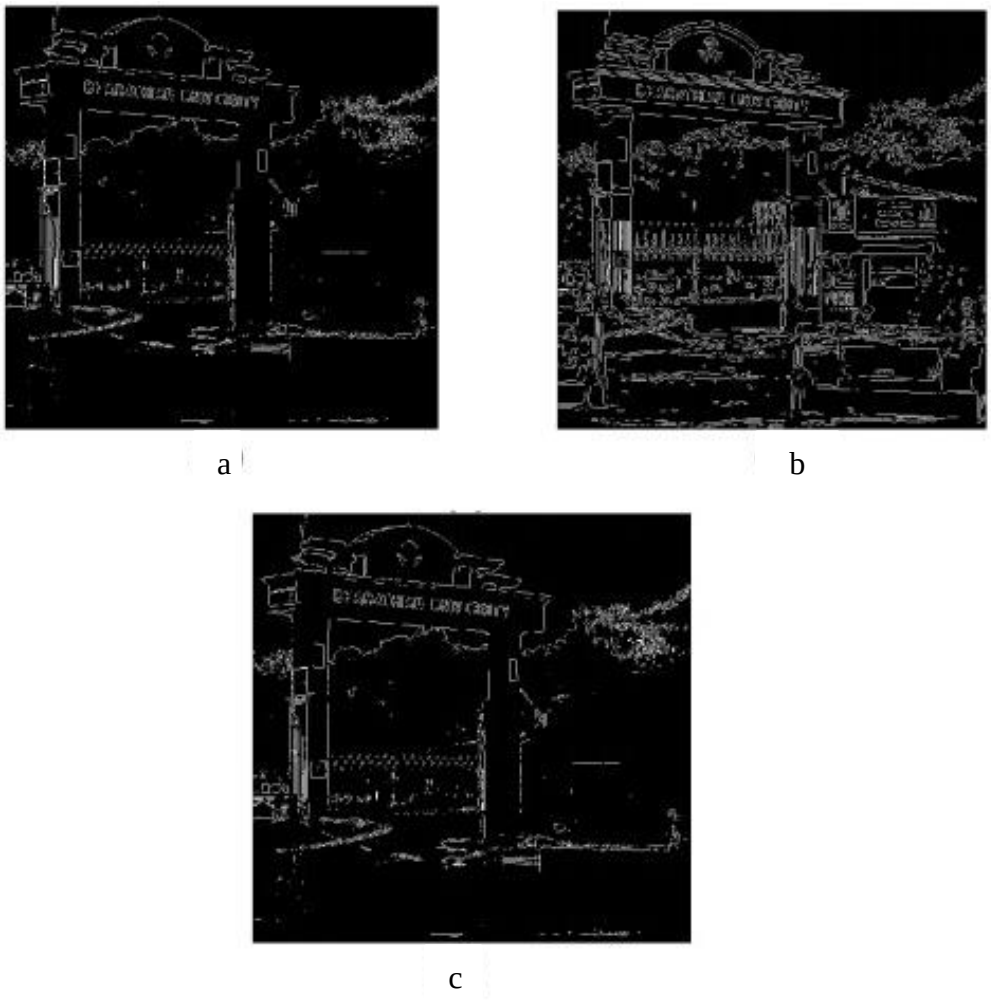

a b c

Figure 2.6: Edge detection metnoas. a) using Prewitt Method, b) using Roberts Method, c) using Sobel Method [14]

## 2.5 Region Growing Methods

Region growing is region based method in segmentation. This method and pixel based method are classified in the same category.

In this method pixels are gathered to take the precise regions. In region growing method seed are playing an important role to extract the specific object which must be segmented. Noise is one of the causes which is effect on choosing the true seeds. In the other words, final results depend on assigning the correct seeds. The algorithm is: [15]

1. Select a seed
2. The region Grows around the seed
3. Selecting another seed from unlabeled pixels
4. Applying region growing in new seed
5. Continue until no region remain.

In figure 2.7 a, PET Image is shown which is contain tumor and b is the segmented image with respect to the region growing algorithm [16].

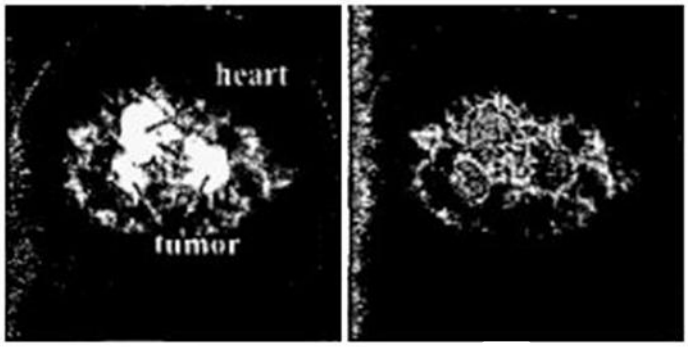


a b

Figure 2.7: a) The original image contains tumor, b) Segmented image by applying region growing method [16]

## 2.6 Graph-based methods

There are numerous methods which are used graph-based segmentation in image analysis such as Random Walker, Normalized Cut clustering, Minimum Cut, Isoperimetric Partitioning and Minimum Spanning tree segmentation [8].

The main aim in this method is to define edges in graph. Nodes which are used in this method are pixels. The difference between pixels is declare as weighted edges, in an image.

Graph based segmentation is used to generate a principle to partition the graph to anticipated clusters. The outcome nodes shows the segmented materials in the image. Following sample show an image segmented using graph based segmentation [17]. In figure 2.8 a, the original image and b, the graph-based segmented image is shown.

a b

Figure 2.8: Original image, b) Graph-based segmented image [17]

## 2.7 Segmentation based on Clustering

Normally Images consist of many objects therefore segmenting all the objects may be a big tragedy. Pixels in the image which are similar to each other and different from the other pixels form a cluster. There are two main groups of algorithm for clustering, hard and soft. In the hard clustering each cluster has a specific data which are just belong to that cluster whereas in soft clustering each data can belong to more than one cluster [18].

In this example the clustering process is shown. Obviously, we can see that the data is segmented to three deferent parts which are identified by three different colors.

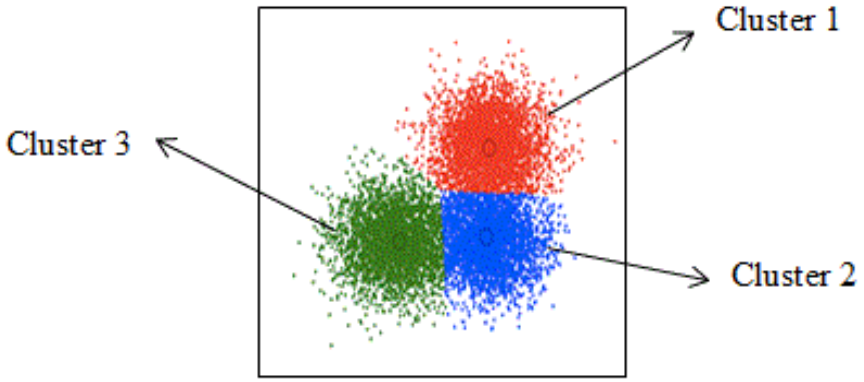

Figure 2.9: Clustering result with 3 clusters

There are numerous Clustering methods which are used in many applications. Plenty of those methods are used in image segmentation. Clustering techniques are divided in to two different parts which are supervised and unsupervised clustering. In the supervised clustering the clustering region is manually defined but clustering criteria is already defined in the unsupervised clustering.

Grouping the image might be based on features or content in the image. Keywords are some features which represent the properties of an image. In Keyword based clustering these features are used to assign a font to describe an image. On the other hand, in content based clustering all the information such as texts and shapes are represented by content. K-means clustering is one of the popular example of the content based clustering [19].

Some of the main clustering method are Relevance Feedback Clustering, Log-based clustering algorithms, Hierarchical clustering Methods, K-means and FCM clustering.

### 2.7.1 Relevance Feedback Clustering

To improve desired enquiry based on low-level properties, Relevance feedback is used. Relevance feedback is a supervised clustering. When this feedback system

identify a likeness in a group of images, by utilizing the most relevant images the system continue to refine the query, although this process can be manually done.

Relevance feedback is a kind of image recovery based on the keywords. This method matches the keyword from the input and the other dataset images. The week point of this method appears when there is not enough keyword to compare and it make the process very challenging [20]. This technique also uses user relevance feedback so as to evade unexpected errors and common redundancy [21]. Naturally a relevance feedback method holds both positive and negative feedbacks which is used in Bayesian classifier [11] while the other clustering methods which are based on content cannot adapt themselves to user modifications [21].

### 2.7.2 Log based clustering algorithms

Retrieval system logs followed by an information recovery process are responsible for image clustering in this technique [4]. For the retrieval system it is required to exude session keys in the current process. The log-based document is generated by cluster in each session which preserves the image similarity. The log-based vector in every session is related to the log-based documents which is received from the cluster [20]. The session cluster is changed by this vector. Consequently, at least one specific document vector might be generated by hybrid matrix with the equivalent log-based vector. The hybrid matrix which is clustered in this process in the outcome of the process. This technique is more complicated in multi-dimensional images [22].

### 2.7.3 Hierarchical clustering Methods

Hierarchical clustering is used in Data mining and statistics. This method is trying to make a hierarchy of the clusters. This method is more expedient for the multi-dimensional images [4]. In this method the series of partitions are running from a single cluster up to the n clusters which are contained an object. Agglomerative

methods are subsets of the hierarchical Clustering. Agglomerative techniques are mostly used and is called “bottom up”. The observation is start from one cluster and continue with the pair of the clusters in next step. This method is represented by dendrogram diagram. Dendrogram defines the association separations in each analysis step which is illustrate as an example given bellow.

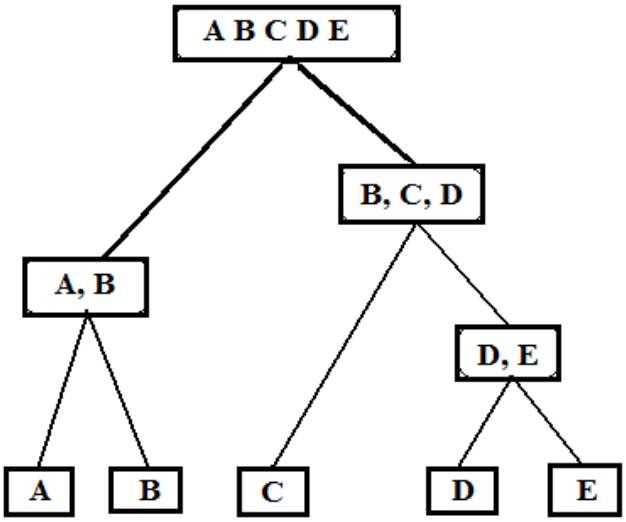

Figure 2.10: Illustrated hierarchical methods.

This clustering process present series of data which are partitioned ($P_n$, $P_{n-1}$, ..., $P_1$). $P_n$ contains n clusters and $P_1$ consists of the group including all n conditions.

Step 1: This process is stated by assigning each of the items to the deferent cluster. Then if we know the number of items for example N, we also have N clusters.

Step 2: Let the similarity between the items and clusters be equal.

Step 3: Find the maximum similarity between the pair of clusters the combine them into a single cluster then one cluster is removed.

Step 4: Calculate the similarity between the new cluster and each of the existing clusters.

Step 5: Repeat step 2 and step 3 until all the clustered items merge into one size N cluster [4].

Another method is divisive hierarchical clustering which its process is the inverse of hierarchical clustering and it is rarely utilized in the applications. Figure 2.11 shows the segmented image using hierarchical clustering method which is divided in to 3 partitions.

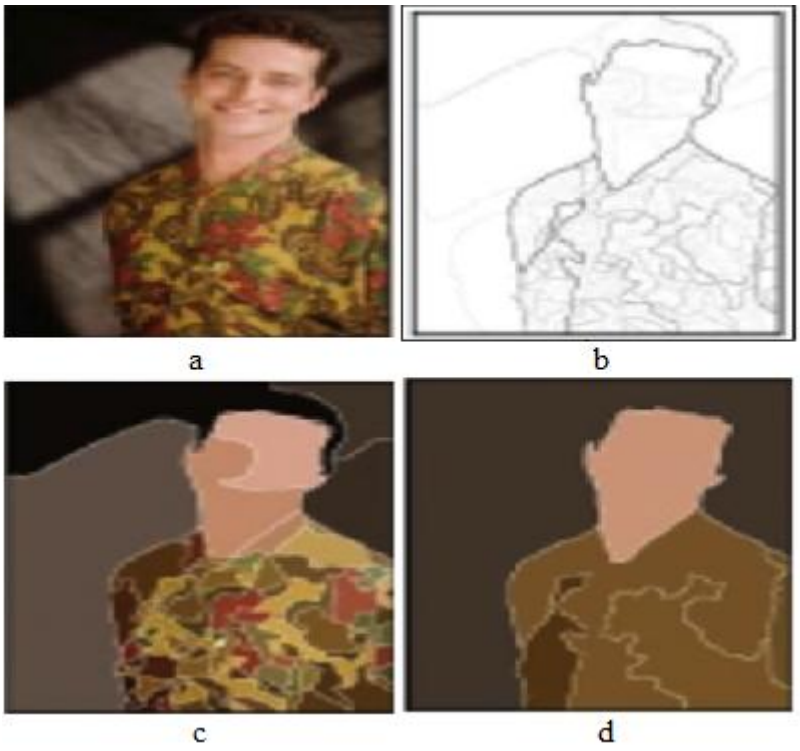


Figure 2.11: a) main image of a man, b, c and d) deferent segmented images by using hierarchical clustering [23]

### 2.7.4 K-means Clustering Algorithm

McQueen [24] in 1967 invented one of the simplest unsupervised clustering algorithms [9], [25], K-means clustering. This method which is used in signal

processing, data mining and image processing, classifies a given data by using certain number of clusters.

In image segmentation the main idea is to find k number of centroid for k clusters (one centroid for each clusters). Because the different location of the centroid may cause different results, centroids should be placed in a tricky way. It is recommended that to place the centroids as far as possible from each other. Furthermore, each point in the data set must be related to the nearest centroid [9]. After assigning all data points to the nearest centroid this process will be repeated by choosing the new centroids. New centroids are calculated by the average of the distance between the specific cluster and belonged centroid [26]. This loop is repeated until the position of the centroid becomes stable [27]. In another word, data vectors in K-means method are divided into predefined and known number of clusters [28] [29].

K-means clustering algorithm has 5 main steps which is illustrated as follows:

Step 1. Number of the clusters must be chosen whether randomly or manually $\mu_i$, $i$= {1, 2, 3…, $k$}

Step 2. Each point $x_j$ must be assigned to the nearest $\mu_i$ to generate k clusters. Thus by using Euclidean distance equation the nearest distance is computed:

$$d_{ij} = \left\| x_j - \mu_i \right\| \tag{2.3}$$

Inputs are $X = \{x_1, x_2, ..., x_n\}$

Step 3. Matrix U must be calculated as follows: $U = [u_{ij}]$, where $u_{ij} \in \{0,1\}$

$$\left\{ \begin{array}{ll} \sum_{j=1}^{k} u_{ij} = 1; & for\ all\ \ j \\ 0 < \sum_{j=1}^{n} u_{ij} < n\ ; & for\ all\ \ j \end{array} \right\} \tag{2.4}$$

Step 4. After calculating the U, new centroid is computed by obtaining the average of all pixels in the cluster and cluster center.

$$\mu_i = \frac{\sum_{j=1}^{n} u_{ij} x_j}{\sum_{j=1}^{n} u_{ij}} \quad ; \quad for \ \ all \ \ i \tag{2.5}$$

Step 5. Since there is a difference between new iteration and the previous iteration, go to step 2 otherwise stop.

The goal is to minimize the distance between clusters point and centroids. The objective function that calculates the square error by using Euclidean distance is shown below:

$$D = \sum_{i=1}^{k} \sum_{j \in c_i} \left\| x_j - \mu_i \right\|^2 \tag{2.6}$$

Where $\left\| x_j - \mu_i \right\|^2$ is a distance between centroid and data point. $c_i$ is the $i$-th cluster and it's centroid is $\mu_i$. Figure 2. 10 shows two different images which is segmented by k-mean clustering with different number of clusters. This example shows that by using more clusters the segmented image is more similar to the original image.

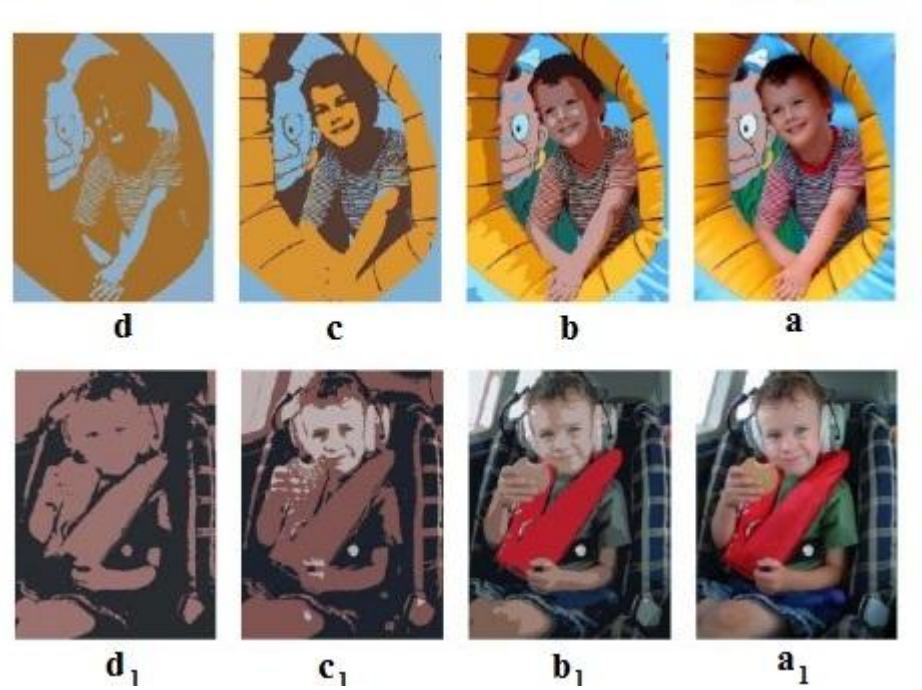

Figure 2.12: a, $a_1$) original images. b, $b_1$) K-means clustering result with k= 10. c, $c_1$) K-means clustering result with k= 4. d, $d_1$) K-means clustering result with k= 2 [29]

The whole k-means process is shown as a flow chart in figure 2, 13.

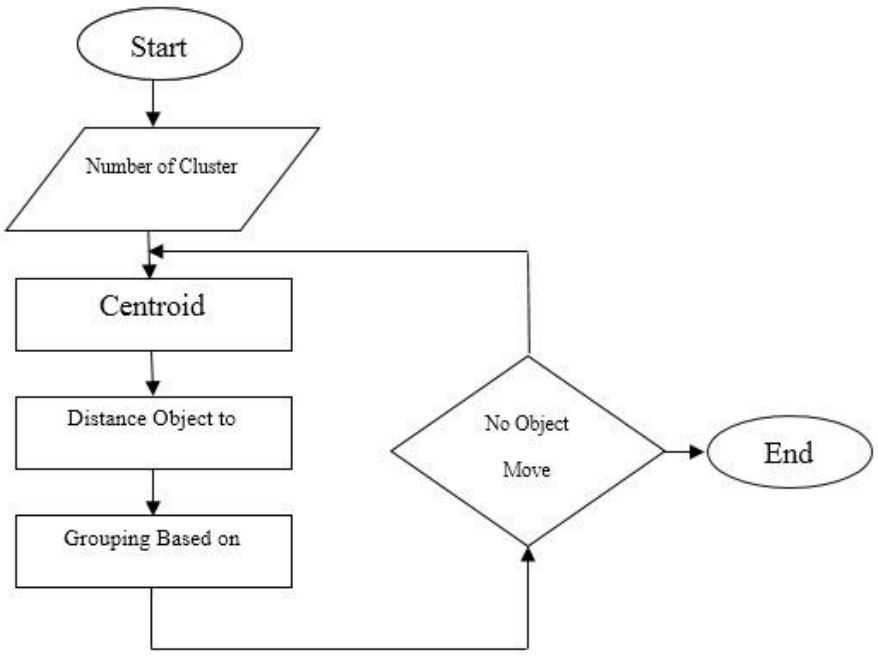

Figure 2.13: K-means clustering algorithm`s block diagram [26]

The method will be clearer by showing its algorithm as follows.

1. Randomly set k points as the clusters centroids.
2. Each data point is assigned to which centroid that has the minimum distance with it.
3. After assigning all the data points to the specific cluster, new centroid must be chosen for each cluster that calculated as the average of the data points' distance in one cluster.
4. Continue second and third steps until centroids movement stops.

Figure 2.14 illustrate the k-mean clustering process in each iteration. In this example, number of the centroids are three. It is obvious that after nine iteration the centroids which are defined by cross, doesn't move anymore and they converge therefore the algorithm is stopped.

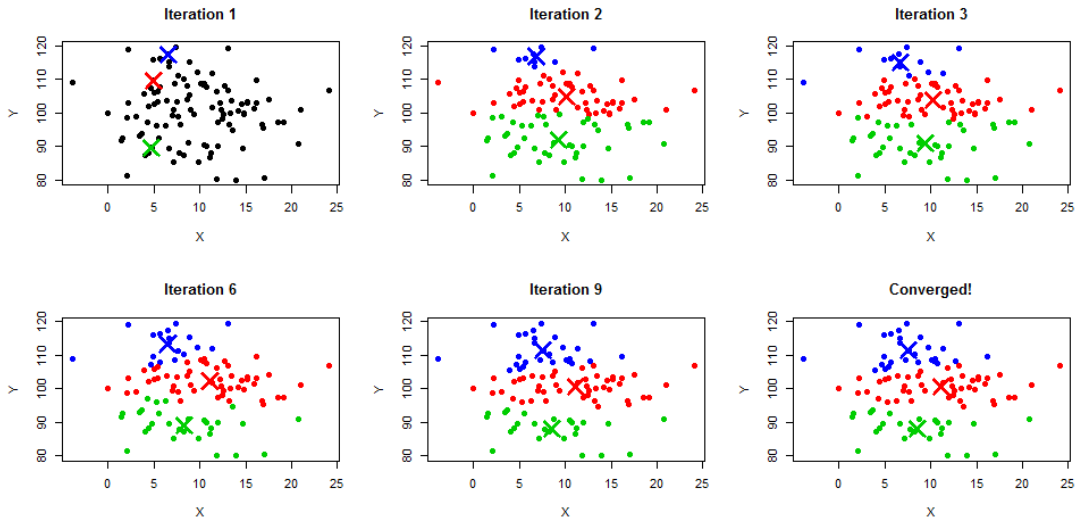


Figure 2.14: K-Means Algorithm performance in different iterations [26]

### 2.7.5 Fuzzy C-means Clustering (FCM) Algorithm

FCM is one of the soft clustering methods which allows a data belong to more than one cluster. Bezdek in 1981 [30], [19], proposed the FCM clustering algorithm. One of the important and most widely used algorithm is Fuzzy C-means algorithm which

is frequently used in image segmentation, medical imaging, pattern recognition and etc.

Fuzzy C-mean clustering divides the samples to c clusters which are already defined. FCM algorithm works by allocating the membership to each data points of each cluster centroid according to the distance between data and clusters. Obviously, summation of membership of each data point should be equal to one.

The algorithm is based on minimizing the objective function which is explained in equation 2.7.

$$J_m(U,v) = \sum_{k=1}^{N}\sum_{i=1}^{c}(u_{ik})^m \|y_k - v_i\|_A^{\,2} \qquad 1 \le m < \infty \tag{2.7}$$

Where $y_k$ is the data, $c$ is the number of the clusters, m is weighting exponent, $U$ is the fuzzy partition of the data $U= [u_{ik}]$, $v_i$ is the center of the $i^{th}$ cluster. In the cluster $i$ the membership has a degree which is $u_{ik}$. $v_i$ is the center of cluster $i$. A is the weight matrix. $Y = \{y_1, y_2, ..., y_k\}$.

The membership will be update with this formula:

$$u_{ik} = \frac{1}{\sum_{j=1}^{c}\left(\frac{\|y_k - v_i\|}{\|y_k - v_j\|}\right)^{\frac{2}{m-1}}} \tag{2.8}$$

And the center of the cluster is:

$$v_i = \frac{\sum_{k=1}^{n} u_{ik}^m x_k}{\sum_{k=1}^{n} u_{ik}^m} \tag{2.9}$$

When $\max_{ik}\left\{\left|u_{ik}^{(k+1)}-u_{ik}^{(k)}\right|\right\}<\varepsilon$ the whole iteration stops. $\varepsilon$ is the limitation principle which is between zero and one. The iteration step is known as $k$ and $u_{ij}$, is a membership of objective function.

The corresponding algorithm for Fuzzy C-means clustering is demonstrated.

1. Set the primary value for *m*, *c*, $U^0$ to predict the initial clusters.
2. Calculate the centroid of the clusters ($v_i$)
3. Update $U^k, U^{k+1}$ (from equation (2.8))
4. If $\|U^{k+1}-U^k\|<\varepsilon$ then STOP, else return back to step 2.

Figure 2.13 shows the result of applying FCM clustering in Lena's image and figure 2.14 illustrate the difference between their histogram. It is clearly show that segmented image divided by 4 different area that contain 4 different intensity.

a b

Figure 2.15: a) 256×256 Lena gray scale image b) segmented image using FCM clustering with (*c*=4)

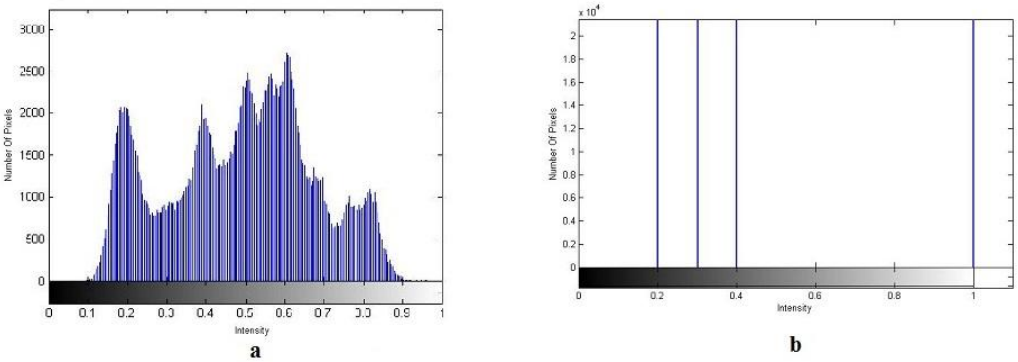


Figure 2.16: Original Lena image histogram b) histogram of the segmented image by FCM clustering

# Chapter 3

# FEATURE EXTRACTION & 3D RECONSTRUCTION

## 3.1 Feature extraction

### 3.1.1 Introduction

Feature extraction includes decreasing the number of resources which are required to define a large amount of data. Different feature extraction method is used for denoising, independent component analysis, dimensionality reduction [31]. Feature extraction in image processing includes Edge detection which is discussed in chapter 2, Corner detection, Blob detection, Ridge detection and etc.

### 3.1.2 Corner detection

Corner detection is a method to extract the specific feature and evolve the content of the image. This method is used in image registration, motion detection, 3D modeling and etc. A corner is defined as a connection between two edges. There are numerous kinds of algorithms for corner detection. One of the most important and frequently used one is Moravec corner detection algorithm [32]. In this algorithm corner is a low self-similarity point. To find the corner, the algorithm checks each pixels of the image. Similarity measurement is computed by considering the sum square difference between the two patches. If the result be lower the similarity is higher.

In figure 3.1 corners which are detected by this method are determined by red points.

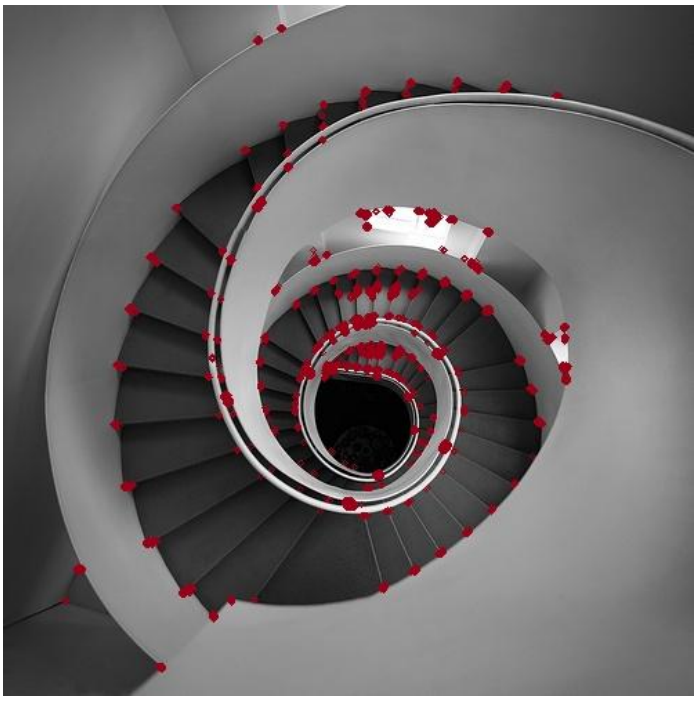

Figure 3.1: Corner detection result displayed by red color [32]

### 3.1.3 Blob detection

Blob detection in image processing is defined as a region detector which that region is different in color or intensity. Blob detectors are representing the additional descriptions of an image structure that edge detectors and corner detectors are not be able to do it.

One of the popular blob detectors is based on the Laplacian of the Gaussian. The input image is *f(x, y)*. By convolving the input image with the Gaussian kernel we have:

$$g(x, y, t) = \frac{1}{2\pi t^2}\, e^{-(\frac{x^2+y^2}{2t^2})} \tag{3.1}$$

Where $t$ is a certain scale to give the scale space representation $L(x, y, t) = g(x, y, t) * f(x, y)$ . After that we apply the Laplacian operator. $\nabla^2 L = L_{xx} + L_{yy}$ is

calculated [62]. In figure 3.2 the area which has different colors after applying blob detection are separated by yellow line.

Figure 3.2: a) original image. B) Partitioned image by blob detection method [62]

### 3.1.4 Ridge detection

Image analysis was the main reason to create the ridge detection and it is used to detect the interior objects which are extended and have a long shape. Ridge-detection is also used in image segmentation in terms of watershed and graph based segmentation [4].

There are three obliging parameters that should be mentioned. These parameters are called Mandatory Parameters which are [33]:

1. Sigma ($\sigma$): This parameter is used for the derivative operation and to control the sigma.
2. Lower Threshold ($T_L$): The points which has a line shape which are the threshold for rejecting the lower value.
3. Upper Threshold ($T_U$): The points which has a line shape which are the threshold for accepting the higher value.
4. Dark line: This parameter shows that line which is selected is dark or bright.

There are some optional parameters in ridge detection which are used to estimate the mandatory parameters [33].

1. Line width ($\omega$): this parameter estimate the $\sigma$ by:

$$\sigma = \frac{\omega}{2\sqrt{3}} + 0.5 \tag{3.2}$$

2. Higher contrast ($C_U$): This parameter seeking for the highest intensity in the line. Thus it estimate the Upper threshold parameter.

$$T_U = [0.17 * \frac{2 * C_U * \frac{\omega}{2}}{\sqrt{2\pi}\sigma^3} * e^{-\left(\frac{\frac{\omega^2}{2}}{2\sigma^2}\right)}] \tag{3.3}$$

3. Lower contrast ($C_L$): This parameter seeking for the lowest intensity in the line. Thus it estimate the Lower threshold parameter.

$$T_L = [0.17 * \frac{2 * C_L * \frac{\omega}{2}}{\sqrt{2\pi}\sigma^3} * e^{-\left(\frac{\frac{\omega^2}{2}}{2\sigma^2}\right)}] \tag{3.4}$$

In figure 3.3 ridge detection result is illustrated.

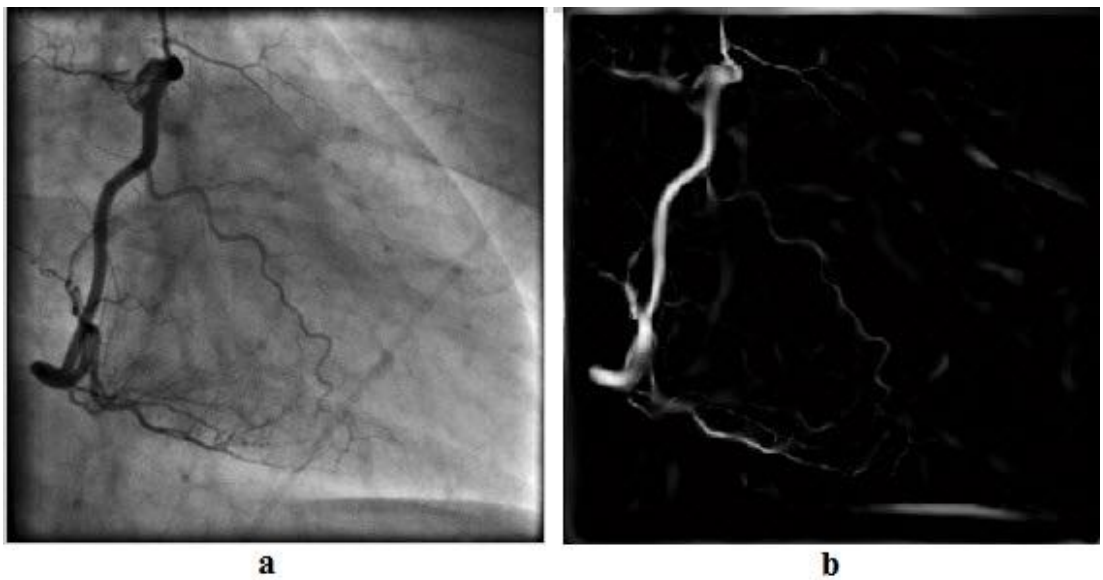

a b

Figure 3.3: a) original vessel image, b) extracted vessel by using ridge detection method [36]

## 3.2 3D Reconstruction

### 3.2.1 Introduction

Visualization is a mapping process from reality in to the couple of numbers (images). 3D visualization is a technique for 3D imaging from 2D images. There are several existing method to visualize the reconstructed images. There are lots of microscopic and macroscopic level applications for 3D reconstruction [34] which are permitted to study very small or very huge objects. Generally to reconstruct the 3D object from 2D images two techniques are used. Volume Rendering and Surface Rendering.

### 3.2.2 Volume Rendering Technique

Volume rendering technique is widely used in medical applications such as cancer detection during the surgery. This technique assign colors to the objects data and visualizes the transparent or opaque of the structures. Figure 3. 4 and 3.5 shows an example of 3D volume rendering result in MR image using transparency and opaque by assigning gray scale and color in to the object.

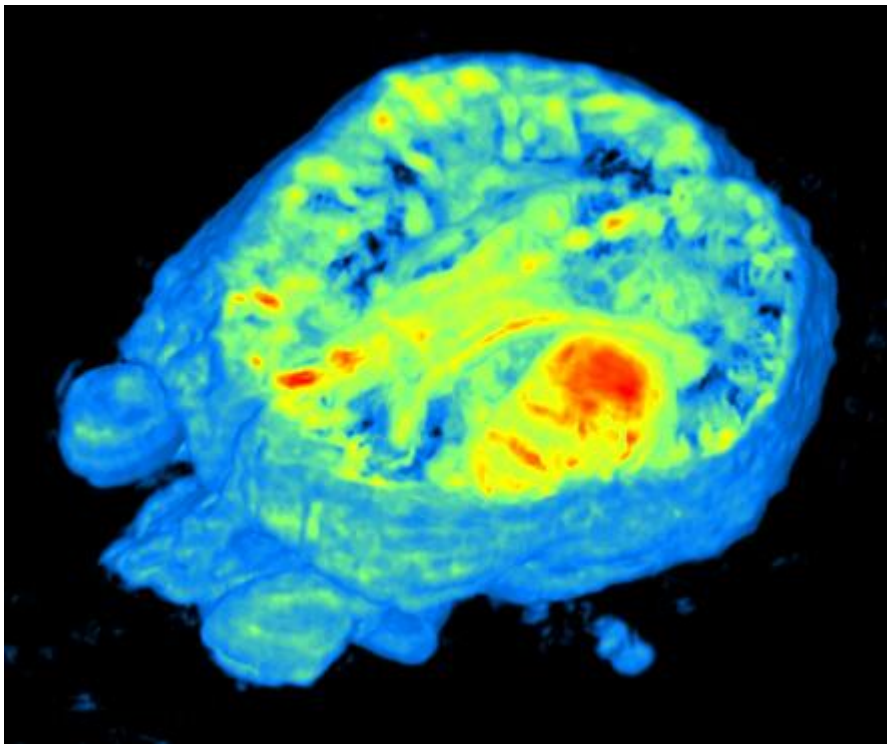

Figure 3.4: 3D volume rendering of the brain MRI which contain tumor by assigning color

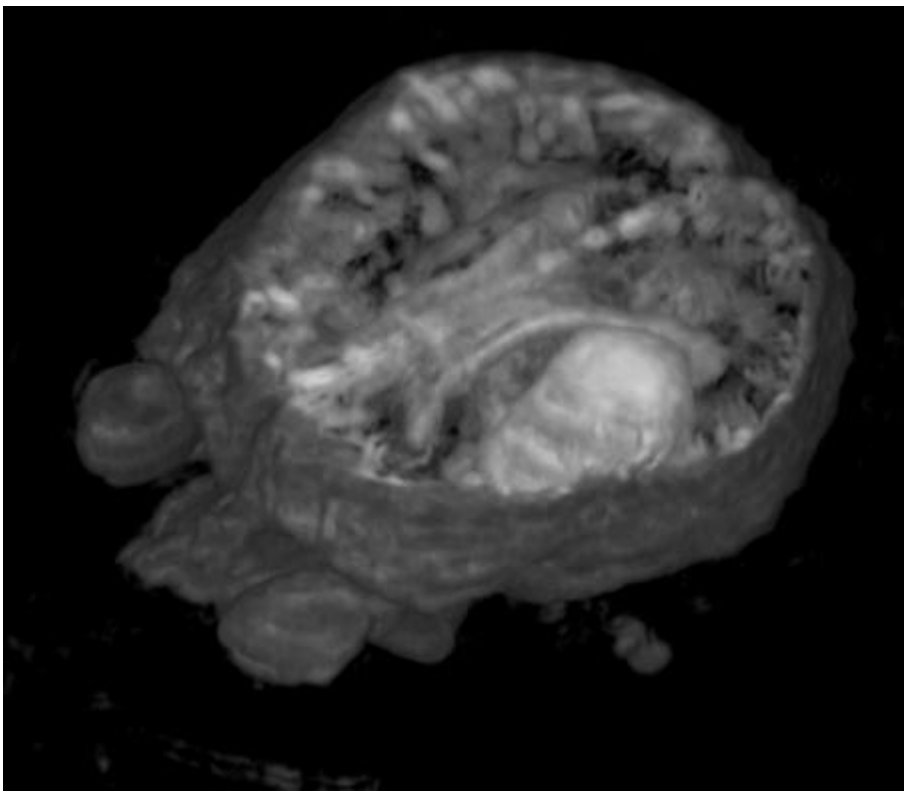

Figure 3.5: 3D volume rendering of the brain MRI which contain tumor by assigning gray scale

### 3.2.3 Surface Rendering Technique

Surface rendering represent a surface visualization of reconstructed object. Surface rendering is depends on the quality of the segmentation. In surface rendering interior elements are not visible. This technique is time consuming. In compare to the volume rendering we can mention that by using volume rendering it is possible to generate immediate 3D model but volume rendering is expensive and needs advanced computer software.

#### 3.2.3.1 Surface rendering using Marching Cube Algorithm

In 3D medical analysis especially in MRI, visualization of the tissue has considerable importance [35]. In 1987 Lorensen and Cline introduced a method to extract the polygonal mesh from a voxels [36].

Marching cube algorithm locates the surface of the volume into the cube which is generated by 8 pixels. This algorithm shows how the surface intersects the cube and marches to the next cube. If the value of the surface that we are constructing is equal or less that the value of the related vertex we assign one to the cube, otherwise the cube receives zero.

To produce Gouraud-shaded object, marching cube algorithm computes unit normal of each triangle vertex. By using the direction of the gradient vector we can obtain the surface normal vector [36].

$$\vec{g}(x,y,z) = \nabla \vec{f}(x,y,z) \tag{3.5}$$

Where $\vec{g}(x,y,z)$ is the gradient vector which is obtained by the derivative of the density function $\vec{f}(x,y,z)$.

# Chapter 4

# THE PROPOSED AUTOMATIC 3D TUMOR SEGMENTATION USING CHARACTRESTICS OF TUMOR

## 4.1 Proposed Tumor Segmentation

### 4.1.1 Introduction

In this thesis, an automatic 3D tumor segmentation based on FCM clustering and characteristics of the tumor is discussed. The proposed 2D Tumor segmentation has three main steps: Slice interpolation, Unsupervised Clustering of the 2D Brain Slices, Feature Extraction from clustered slices. Figure 4. 1 illustrates the diagram of the proposed 3D brain tumor segmentation method.

### 4.1.2 2D Slice Interpolation

In this thesis, a database of MRI dataset with 40 slices for each subject from Cancer imaging Archive [37] are used. Data set which is shown in figure 4. 3, contains 40 slices from T2 -weighted MR Images which contain tumor that are used in our experiments. The reason to use T2 -weighted images is that the tumor is brighter than the other parts of the brain [38].

Obviously, having more slices lead us to reconstruct a clearer and more reliable 3D tumor [39]. Due to limited number of slices in MRI scans, predicted intermediate slices from the real slices using interpolation is proposed to increase the number of slices to improve reconstruction. In this regard, this thesis proposes the shape-based bilinear interpolation [40] to predict more slices.

Suppose that we are going to find the value of a function *f* at the specific point and we already know the value of the function *f* in four different points. Therefore, to calculate the bilinear interpolation firstly we need to compute linear interpolation in both *x* and *y* directions [41]. It is assumed that we know that the value of function *f* at 4 different points $Q_{11} = (x_1, y_1)$, $Q_{12} = (x_1, y_2)$, $Q_{21} = (x_2, y_1)$, and $Q_{22} = (x_2, y_2)$.

$$f(x, y_1) \approx \frac{x_2 - x}{x_2 - x_1} f(Q_{11}) + \frac{x - x_1}{x_2 - x_1} f(Q_{21}) \tag{4.1}$$

$$f(x, y_2) \approx \frac{x_2 - x}{x_2 - x_1} f(Q_{12}) + \frac{x - x_1}{x_2 - x_1} f(Q_{22}) \tag{4.2}$$

Then we calculate the *f* function in *y*-direction.

By applying this method between 2 slices respectively we obtain predicted slice. This process repeated until the targeted number of slices is reached. Figure 4. 2 illustrates the Intra slices (I), Predictive Slices (P) and Bi-predictive slices (B). The result of slice interpolation is shown in figure 4.4.

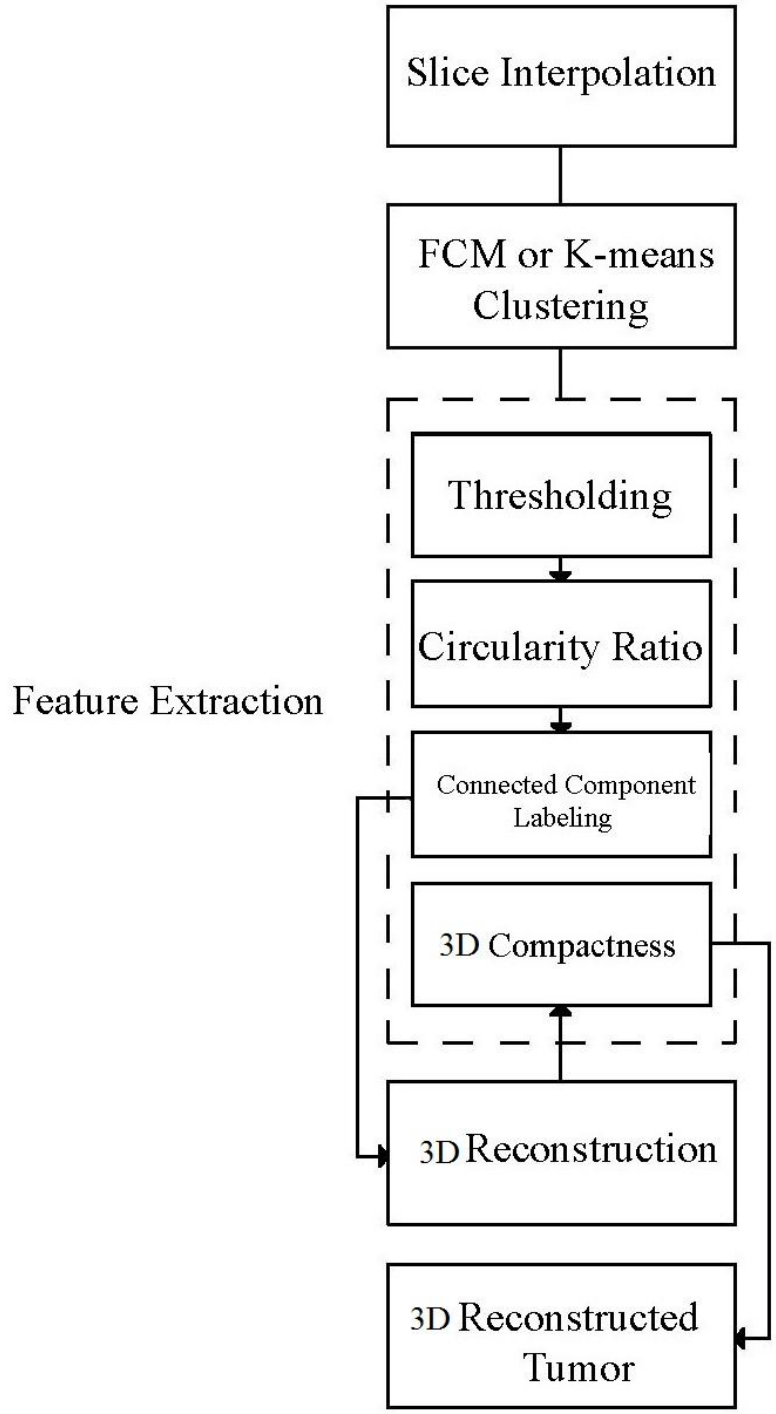


Figure 4.1: 3D Brain Tumor Segmentation Block Diagram

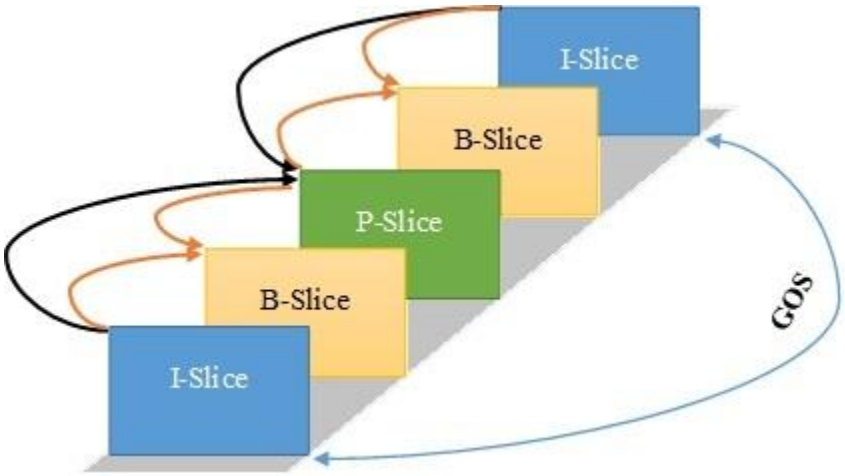


Figure 4.2: Illustration of Intra slices (I), Predictive Slices (P) and Bi-predictive slices (B) of MRI. GOS is one group of slices which is shown by blue 2 sided arrow

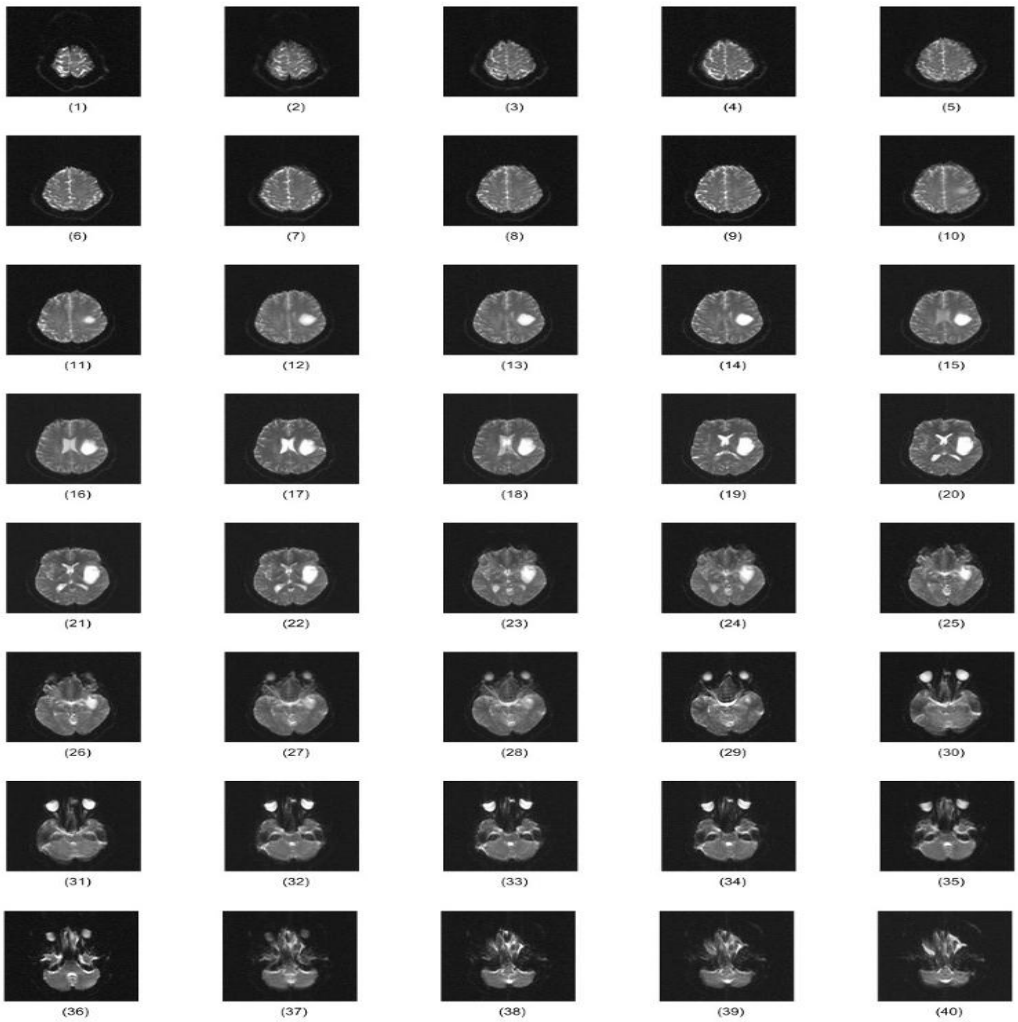


Figure 4.3: 2D MRI brain slices dataset

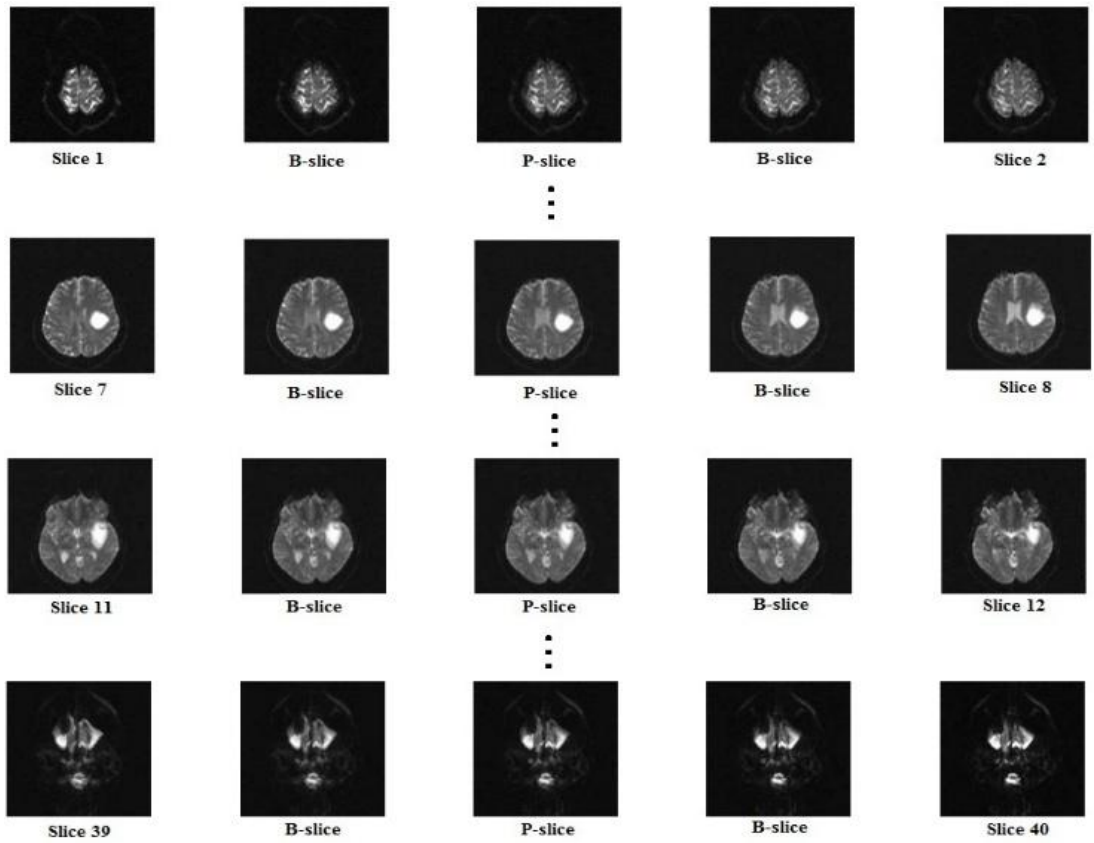

Figure 4.4: The results of Interpolation between slices

## 4.2 Clustering of the 2D Brain Slices

### 4.2.1 K-means Clustering

K-means is an unsupervised technique [42], [43] that classify the given data set in to k clusters (k-clusters). In this experiment k=4. In this section each slice is segmented through the K-mean clustering algorithm. This algorithm divides all the gray levels to 4 clusters and segments them separately.

### 4.2.2 FCM Clustering

By applying FCM clustering each image (slice) segmented in to c partitions which is called clusters. In this experiment c=4. FCM detect the intensity of each pixel in the slice and assign it to a cluster. The results show that clustered image using FCM is clearer than applying k-mean clustering.

## 4.3 Feature Extraction from Clustered Slices

In This part the main aim in to detect the tumor area from clustered slices. Feature extraction needs knowledge of object characteristic [44]. In this approach, Intensity, Circularity [45] and 3D Compactness [46] of the tumor are taking to account.

First of all, the brightest areas of the MR slices will be extracted. For this purpose, it needs to review the Histogram Of the slices and by the helps of Thresholding method [47] the areas with the maximum intensity is detached. To detach the region of the interest it needs to choose the belonged label of that area from its clustered image.

$$T = \begin{cases} 1 & if \quad I_{r_{x,y}} > T_r \\ 0 & if \quad I_{r_{x,y}} \leq T_r \end{cases} \tag{4.3}$$

Where in equation 4.3, $T$ is binary outcome of the thresholding process. $I_{r_{x,y}}$ is the intensity of the pixels in each slice and $T_r$ is the thresholding value which is calculated for higher gray level.

### 4.3.1 Circularity Ratio ($C_r$)

Circularity Ratio is the ratio between the area of circle and the examined object. For example $C_r$ for regular circle is 1, for square is 0.79 and for triangle is 0.61 [48].

$$C_r = \frac{4\pi A}{p^2} \tag{4.4}$$

In equation 4.4, $C_r$ is the circularity ratio, $A$ is the area of the object and p is the perimeter of it. To calculate the circularity of each component of the segmented image that had the highest intensity in the main slice, we must be able to extract all the components from the image. It will get executed by using Connected Component labeling [49].

### 4.3.2 Connected Component labeling (CCL)

Connected Component labeling (CCL) method assigns different labels to every connected component in a given binary image. Following explanation is the way that CCL of the binary image works.

First step is started from finding the first pixel in the image. Then if the pixel not already labeled set a label to it and go to the next step. Based on the connectivity of the component searching for its neighbors will start and then repeat this part until no more connected neighbors remain. Finding next pixel is the next step and doing all above steps until every connected component has unique label. After applying CCL, we can easily extract the components and measure the circularity ratio of the connected components.

### 4.3.3 3D Compactness ratio ($\mathbf{C_R}$)

Compactness ratio ($C_R$), is a dimensionless quantity that measure the rate to which a shape is compact [64]. If a shape is convex, concave or has a distortion in its surface, the compactness ratio will change. $C_R$ is maximized on a sphere [66]. For a 3D object compactness relates the enclosing surface area with the volume [65] and its formula is shown in equation 4.5:

$$C_R = \frac{A^3}{V^2} \tag{4.5}$$

Where $C_R$ is the Compactness ratio, $A$ is the enclosing surface area of the object and $V$ is its volume. In section 4.3 it is mentioned that the Intensity, Circularity and 3D Compactness are the three selected factors to automatically detect the tumor from the other components of the brain in MR images. The third factor, Compactness ratio is calculated for all of the 3D connected components, and the component with highest compactness ration is regarded as the 3D tumor to be segmented.

## 4.4 3D reconstruction and visualization

There are various methods to reconstruct 3D structures form 2D slices. Figure 4.5 shows the slices in matrix form in 3D reconstruction process. The process involves mapping of 2D slices from consecutive 2D space to the 3D space ($\mathbb{R}^2 \rightarrow \mathbb{R}^3$). Two famous methods are volume rendering and surface rendering [45], [50], [51].

Volume rendering, create a direct 3D visualization from the voxels. In another words, it displays the intensity of the voxels in 3D. Volume rendering is performed by assigning a color and opacity value to all pixels and projecting them directly into the image plane without utilizing polygons. On the other hand, 3D surface rendering is based on creating a 3D surface model from contours or boundary lines of 2D slices.

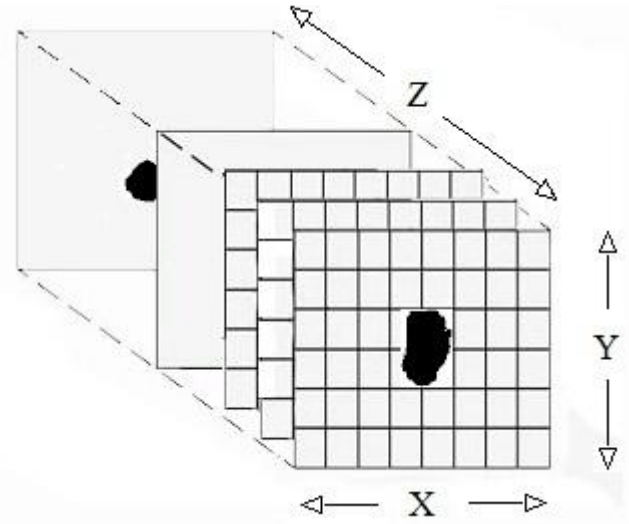


Figure 4.5: 3D reconstruction of 2D images as a matrix form

First step is to find the contour of the ROI in each slice. Second step involves calculating the area of the desired region $\{S_1, S_2, S_3, \ldots, S_N\}$ for all slices. In the third step the volume between two slices are computed. Equation 10 shows how this volume is calculated by using Truncated Cone formula.

$$v_d = \frac{1}{3} \times H \times (S_n + \sqrt{S_n \times S_{n+1}} + S_{n+1}) \quad (4.6)$$

Where the $H$ is the distance between two slices. $S_n$ and $S_{n+1}$ are the area of the interest in two consecutive slices. Step 4 calculates the reconstructed volume by using the following equation.

$$V = \sum_{n=1}^{N-1} v_d \quad (4.7)$$

$v_d$ is the volume between slices. $N$ is the number of slices, $n = 0, 1, ..., N$. Because of the limitation of the slices it is not possible to create a clear 3D visualization of these contours. Therefore, same distance, *H*, must be assigned to each slice used in equation 4.6.

This thesis used 3D surface rendering technique to generate 3D smooth visualization of the brain tumor. Thus, Marching Cube Algorithm is utilized.

After reconstructing the 3D volume, surface rendering procedure is utilized to generate better visualization of small details in the 3D reconstructed structure. In this process, the 3D surface is modelled by using triangular and polygonal faces. The faces are closed set of edges and the polygons are coplanar set of faces [52]. By using 3D surface model we can merge the multiple close components together.

Figure 4. 6 illustrates the details of the proposed method to segment 3D tumor from the given slices by using interpolated slices (i.e. P and B slices) and 3D surface rendering using K-means and FCM based approaches.

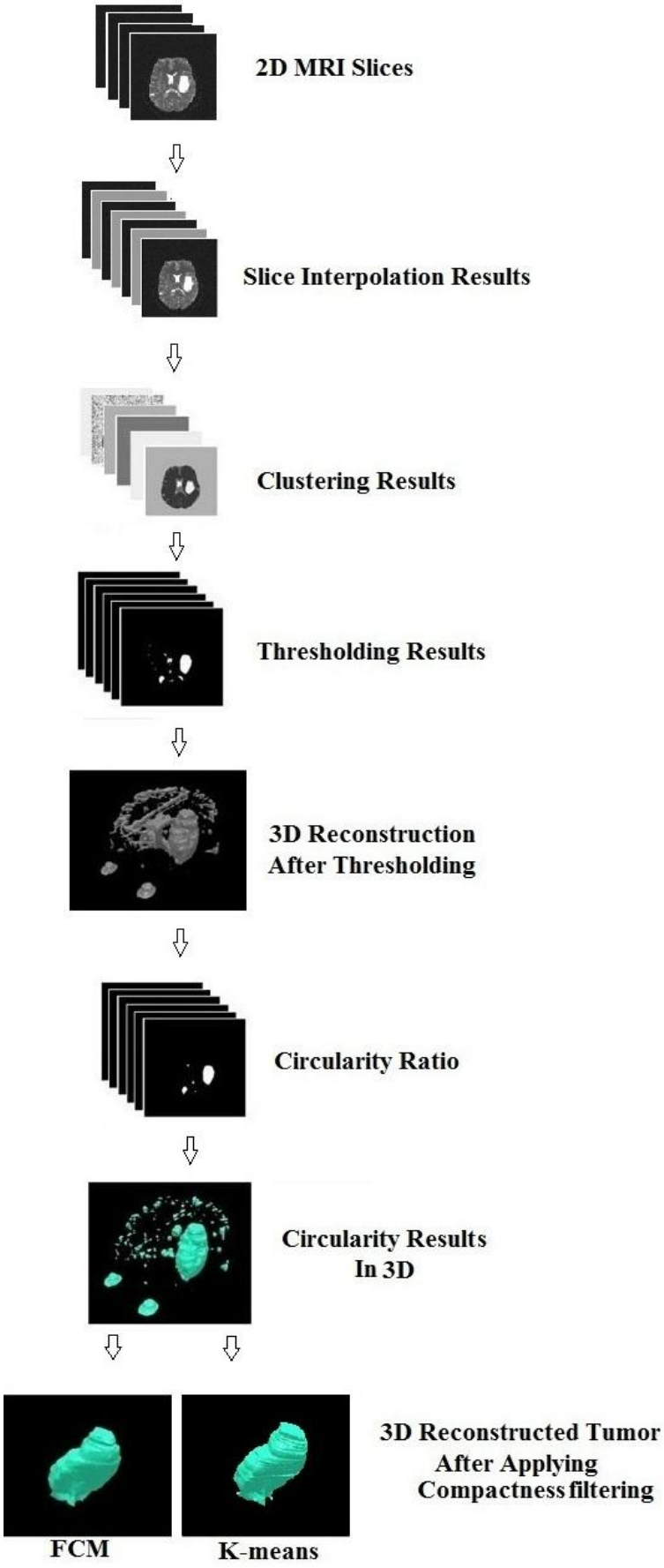


Figure 4.6: Step by Step details of proposed 3D tumor Segmentation method

# Chapter 5

# EXPERIMENTAL RESULTS AND DISCUSSIONS

## 5.1 Introduction

In this chapter the experimental results, block diagrams and figures of the proposed methods are presented. The FCM method is tested in more than one hundred slices from MR T2-w images.

This thesis presents the 3D tumor segmentation and detection using K-mean and FCM algorithm. 3D representation of the tumor plays a crucial fundamental role in medical imaging. Comparison of these two clustering methods impart that FCM method is more sensitive to the alternation of the intensity and the segmented tumor in 2D is more similar to the ground truth. In this chapter the experimental results, block diagrams and figures of the proposed methods are presented.

## 5.2 Experimental Methodology

To qualitative observation, quantitative comparison is also required to measure the performance of the proposed 3D tumor segmentation method. In this respect, the following segmentation metrics are used [53].

### 5.2.1 Sensitivity, Accuracy, Specificity & Precision of the proposed method

In any experiment usually there are some tradeoff between measures. The performance of the proposed method compare to the Ground truth data examined as follows:

True Positive (TP): Tumor pixels correctly diagnosed as a tumor.

False Positive (FP): Non-tumor pixels incorrectly diagnosed as a tumor.

True Negative (TN): Non-tumor pixels correctly diagnosed as non-tumor pixels.

False Negative (FN): Tumor pixels incorrectly diagnosed as non-tumor pixels.

Sensitivity, accuracy, specificity [54] and precision [55] are defined as follows:

$$Sensitivity = \frac{n_{TP}}{n_{TP} + n_{FN}} \tag{5.1}$$

$$Accuracy = \frac{n_{TP} + n_{TN}}{n_{TP} + n_{TN} + n_{FP} + n_{FN}} \tag{5.2}$$

$$Specificity = \frac{n_{TN}}{n_{TN} + n_{FP}} \tag{5.3}$$

$$Precision = \frac{n_{TP}}{n_{TP}+n_{FN}} \tag{5.4}$$

In all equations above "*n*" represents the number of pixels. The results of FCM and K-means based segmentation methods are given in Table 5.1. Figures 5.1, 5.2, 5.3 and 5.4 show Sensitivity, Accuracy, Specificity and Precision of proposed methods using FCM and K-means clustering. The results indicate that FCM is superior to K-Means based segmentation approach. Accuracy of the proposed FCM based method is higher that all the methods reported in the table 5.1. Furthermore, the proposed method has a higher specificity compared to Texture Features Extraction.

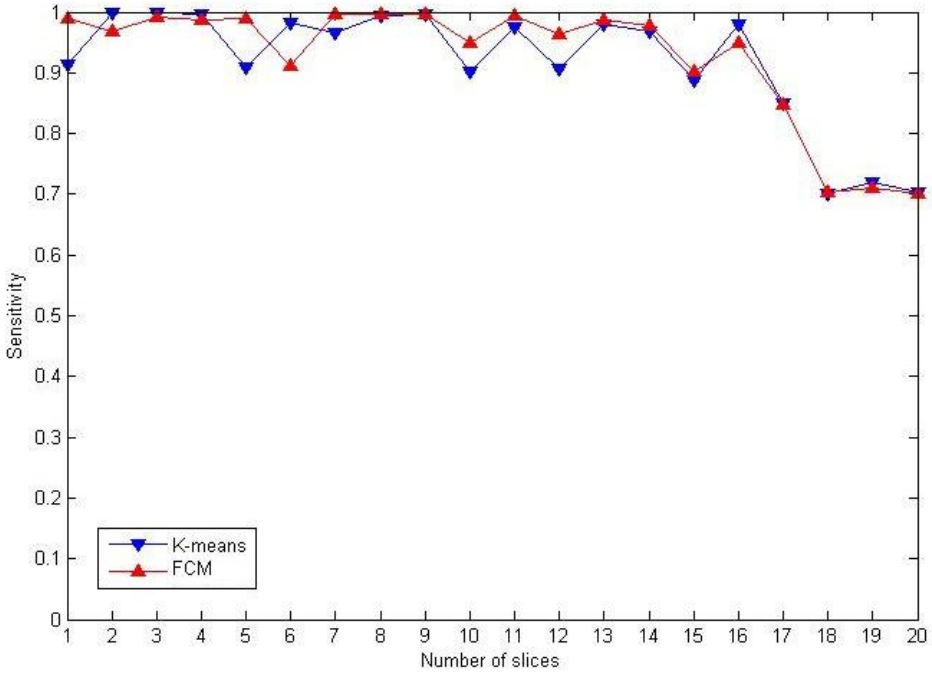


Figure 5.1: The Comparison between Sensitivities of applying FCM and K-means for 3D segmentation

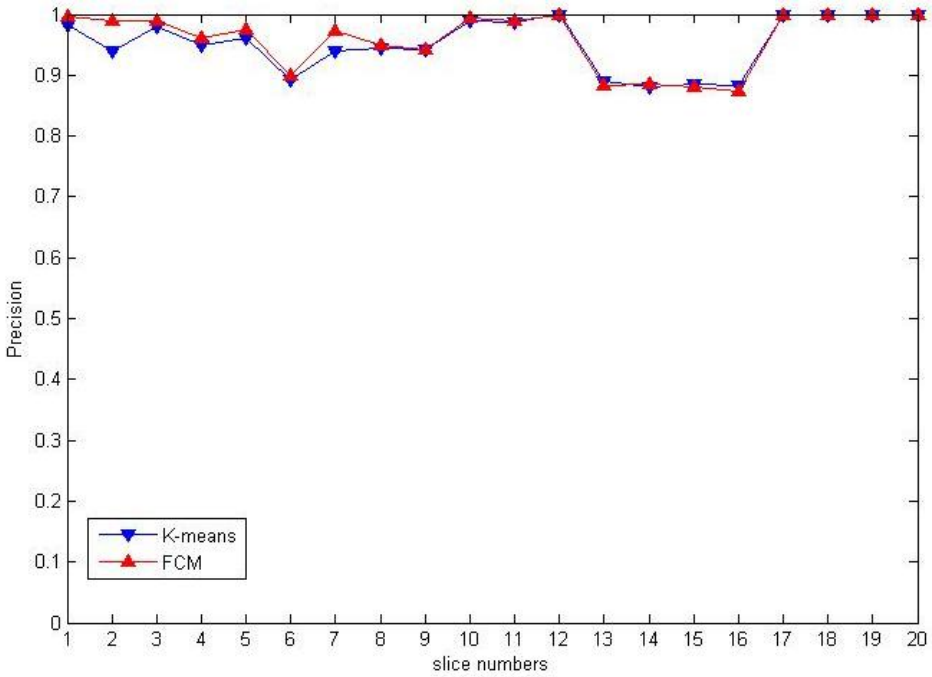


Figure 5.2: The Comparison between Precision of applying FCM and K-means for 3D segmentation

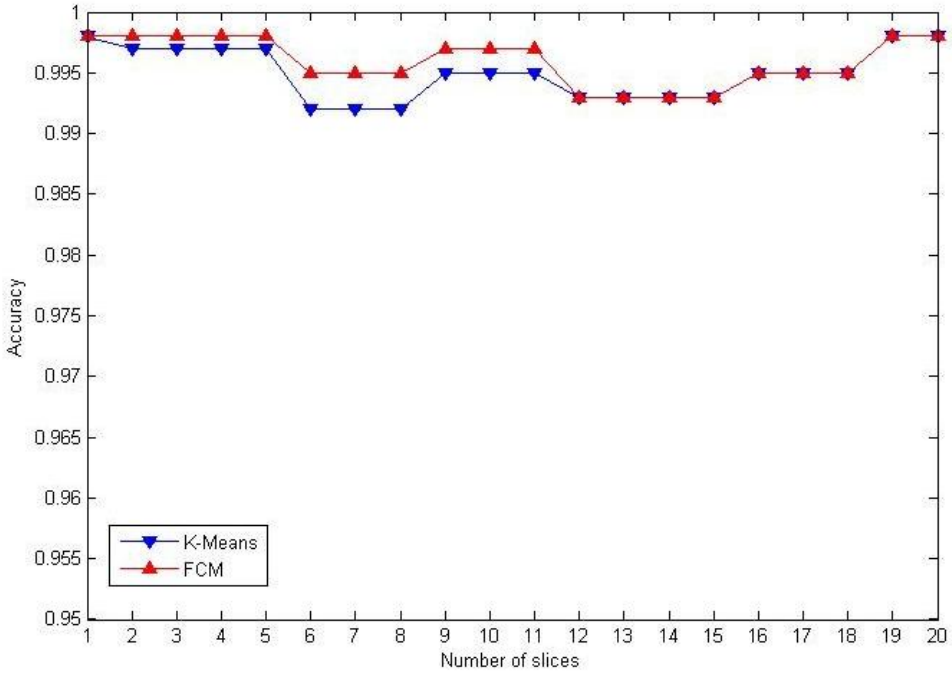


Figure 5.3: The Comparison between Accuracy of applying FCM and K-means for 3D segmentation

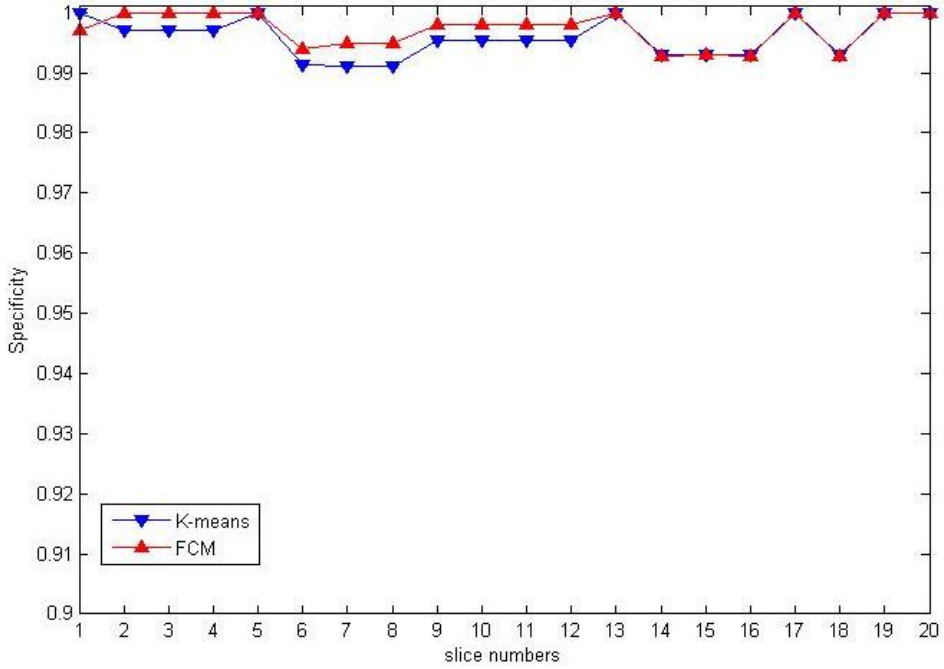


Figure 5.4: The Comparison between Specificity of applying FCM and K-means for 3D segmentation

Table 5.1: Comparing the results between different segmentation Methods

| Method | Sensitivity | Specificity | Precision | Accuracy |
|---|---|---|---|---|
| **Proposed Method with FCM** | 0.925 | 0.998 | 0.957 | 0.996 |
| **Proposed Method with K-Means** | 0.916 | 0.997 | 0.952 | 0.995 |
| Texture Features Extraction [63] | 0.846 | 0.884 | -- | 0.67 |
| Kernel feature selection[56] | 0.969 | -- | -- | -- |
| An improved level set [57] | 0.967 | -- | -- | -- |
| Neural network [58] | 0.960 | -- | -- | -- |
| SVM [59] | -- | -- | -- | 0.989 |
| SVM method [60] | -- | -- | -- | 0.972 |

In addition, the sensitivity, accuracy, specificity and precision of proposed methods using FCM and K-means clustering for the P-slices are compared. The results in figure 5.5- 5.8 shows that sensitivity, accuracy, specificity and precision of FCM clustering for P-slices are also higher than the results for K-means clustering. The performance of two methods is shown with two red and blue colors.

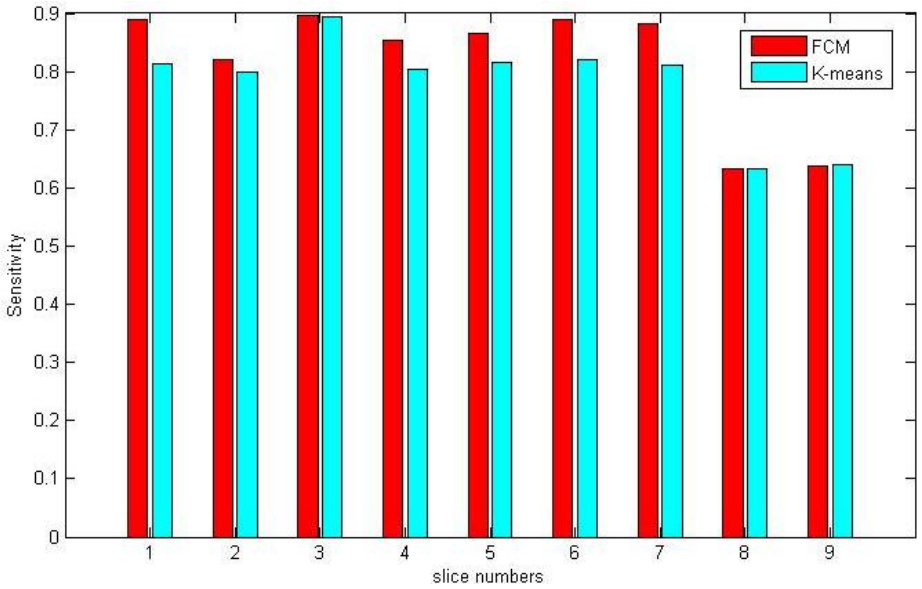


Figure 5.5: The Comparison between Sensitivities of P-slices by applying FCM and K-means

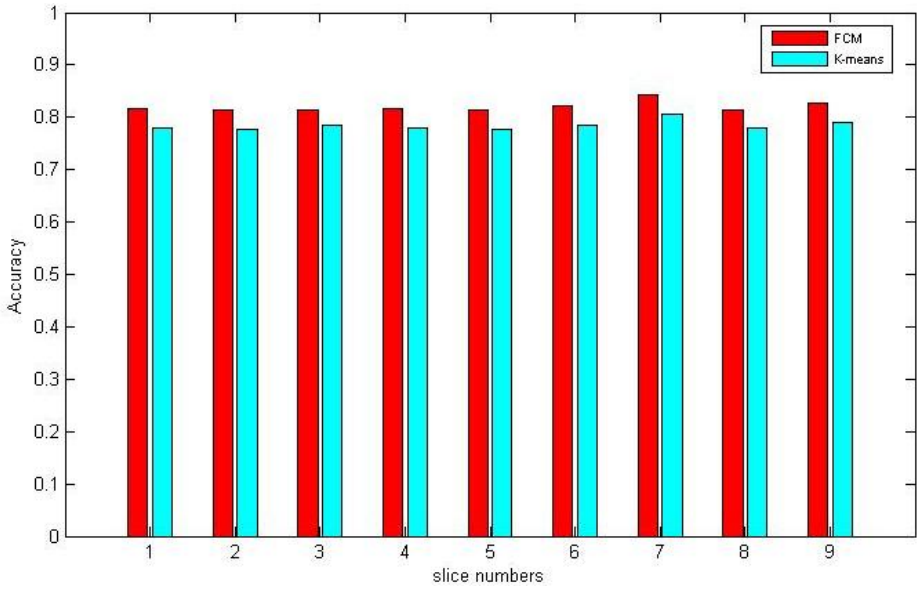


Figure 5.6: The Comparison between Accuracy of P-slices by applying FCM and K-means

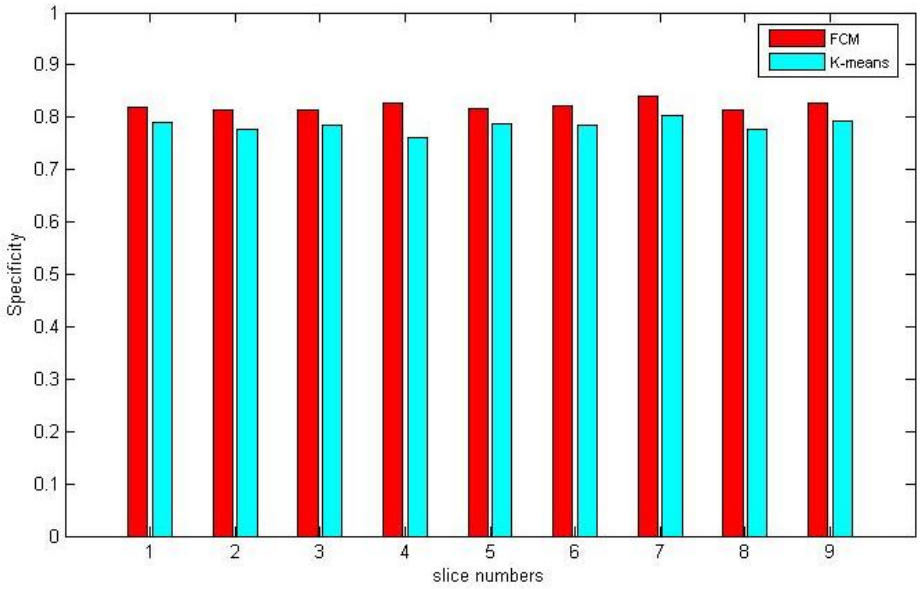


Figure 5.7: The Comparison between Specificity of P-slices by applying FCM and K-means

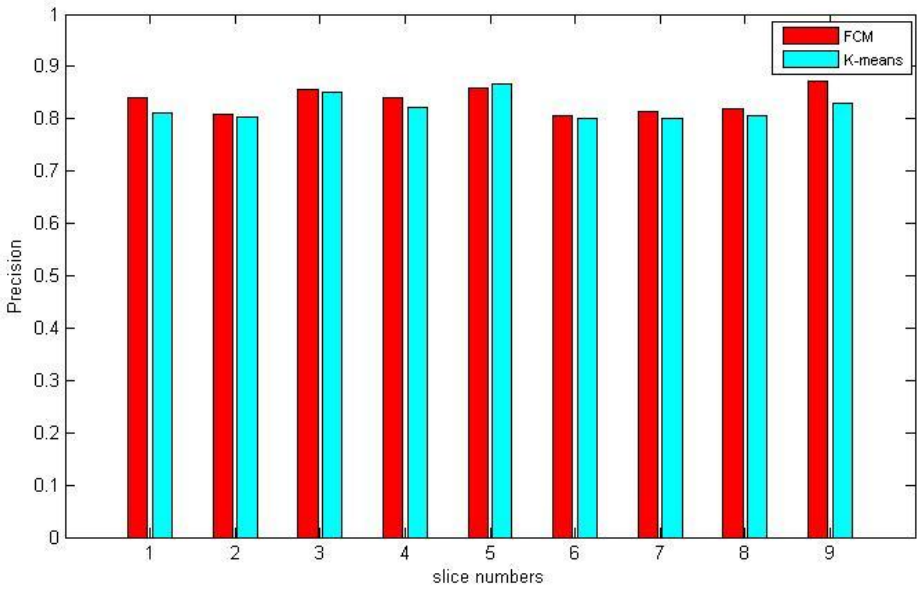


Figure 5.8: The Comparison between Precision of P-slices by applying FCM and K-means

Furthermore, the average of the FCM and K-means performance for I-slices is compared with the FCM and K-means performance for P-slices, which is shown in table 5.2.

Table 5.2: Comparison of K-Means & FCM performance for I-slices and P-slices

| Method | Sensitivity | Specificity | Precision | Accuracy |
|---|---|---|---|---|
| **Proposed FCM Method for I-slices** | 0.925 | 0.998 | 0.957 | 0.996 |
| **Proposed FCM Method for P-slices** | 0.824 | 0.821 | 0.841 | 0.82 |
| **Proposed K-Means Method for I-slices** | 0.916 | 0.997 | 0.952 | 0.995 |
| **Proposed K-Means Method for P-slices** | 0.794 | 0.784 | 0.82 | 0.784 |

The results shows that the performance of the proposed method for the I-slices is higher than the P-slices. In another words, the predicted slices have lower similarity to the GTD in compare with the similarity of the Intra slices and GTD.

### 5.2.2 3D reconstruction Results

The Compactness ratio results of the segmented tumor is given in Table 5. 3. Table shows that the compactness of the 3D segmented tumor which is reconstructed by using interpolation method is closer to the ground truth (GT) in compare to the 3D segmented tumor without using interpolation. In order to compare the performance of the 3D reconstruction process, Ground Truth Data (GTD) which is the manually segmented tumor in each slice by medical experts is used. The distance between slices can be adjusted by changing the number of interpolated slices. Therefore, according to the ratio between number of slices before and after slice interpolation, distance between slices for a constant volume is calculated. For example, $H_1=3.3H_2$, where $H_1$ is the distance between slices before interpolation and $H_2$ is distance between slices after interpolation.

Table 5.3: Compactness Ratio of the Segmented Tumor

| Method | $C_R$ Manual | $C_R$ without Interpolation | $C_R$ with interpolation |
|---|---|---|---|
| **Doctor** | 77.72 | -- | -- |
| **FCM** | -- | 22.90 | 74.72 |
| **K-means** | -- | 22.56 | 74.60 |

Figure 5. 9 shows that in the case of slice interpolation the 3D reconstructed Tumor is smoother and hence has higher Compactness ratio.

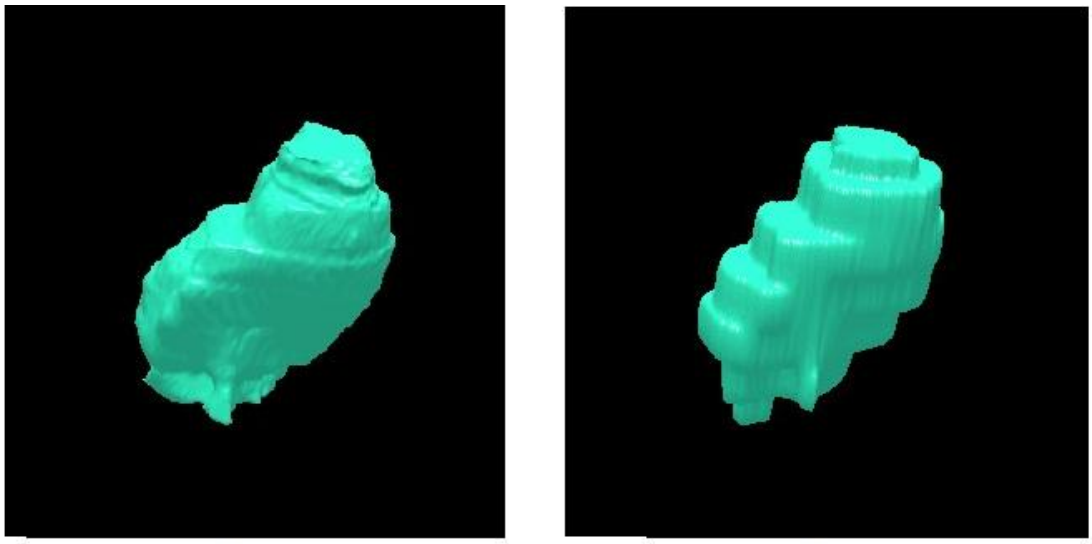


Figure 5.9: 3D Segmented Tumor using FCM with interpolation a) and without interpolation b)

In the following, the visual results of the 3D tumor reconstruction for 3 more samples is shown in figure figures 5.10, 5.11 and 5.12.. In each result, the reconstructed tumor with slice interpolation and without interpolation is compared.

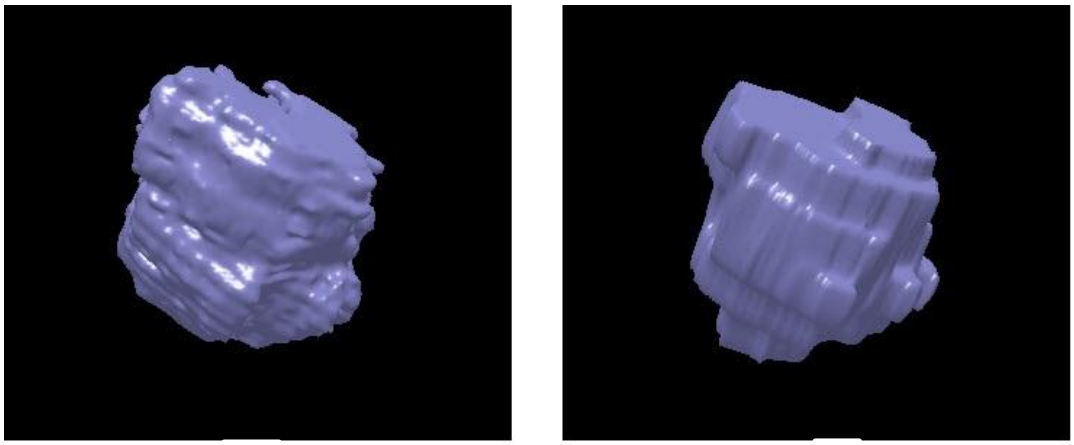

a b

Figure 5.10: Sampıe 2 results. a) 3D Segmented Tumor using FCM with interpolation and b) without interpolation

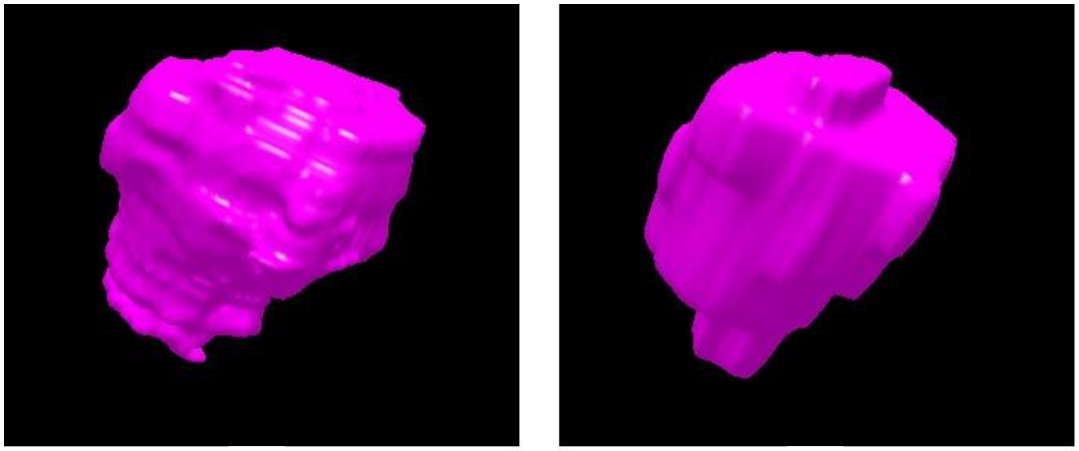

a b

Figure 5.11: Sampıe 3 results. a) 3D Segmented Tumor using FCM with interpolation and b) without interpolation

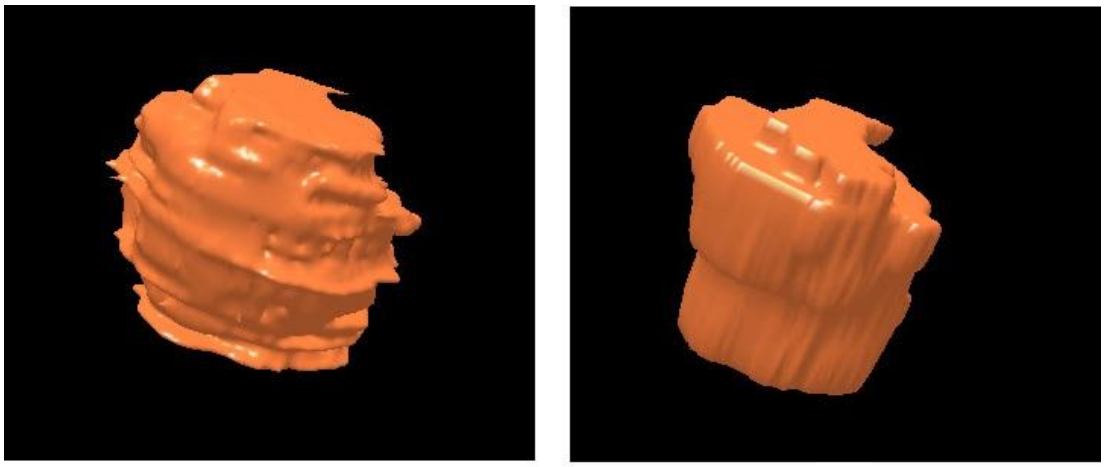

a b

Figure 5.12: Sampıe 4 results. a) 3D Segmented Tumor using FCM with interpolation and b) without interpolation

# Chapter 6

# CONCLUSION

## 6.1 Conclusions

In this thesis is used FCM clustering in 2D for all MR slices to segment the tumor area. 3D reconstructed tumor is generated by the 2D segmented slices through the rendering process. 3D surface rendering technique is used to make clearer reconstructed tumor. In order to produce a perspicuous 3D structure of the tumor and because of the limitation of the 2D MR slices, this thesis proposes slice interpolation to generate more slices between the existing slices. In another words, by applying interpolation between intra slices predictive slices is generated and by using interpolation between predictive slices bi-predictive slices is constructed.

This thesis also proposes tumor segmentation by using characteristics of the tumor in T2-weighted MR images such as intensity, circularity and 3D compactness. This approach leads to achieve higher performance of 3D reconstructed tumor which helps doctors to detect the shape of the tumor specially in the fields of Robotic surgery.

## 6.2 Future Work

There are several future works to explore with respect to the automatic 3D reconstruction of the brain tumor. Improving each sections of proposed method could improve the final result. In this thesis labeling of the slices is depended on the thresholding. Therefore improving the accuracy of the thresholding method might

lead to enhance the quality of the reconstructed tumor. In addition, segmentation of the brain tumor could be developed to segment the different tumor ingredients such as edema and necrosis. Furthermore, the proposed method could be used T1-w MR image as well.

# REFERENCES

[1] Hornak, J. (1996-2014). The Basics of MRI.

[2] Peng, W., Kai, X., Yunping, Z., & Chao, W. (2012). Brain Tumors Classification Based on 3D Shape. *Springer-Verlag Berlin Heidelberg*, 160, 277-283.

[3] Sodek, K., Ringuette, M., & Brown, T. (2009). Compact spheroid formation by ovarian cancer cells is associated with contractile behavior and an invasive phenotype. *National Center for Biotechnology Information, U.S. National Library of Medicine*. 124, 2060–2070.

[4] Fu, K., & Mui, K. (1981). A survey on Image Segmentation Through Clustering. 13, 3-16.

[5] Herman, G., Vase, W., Gomori, M., & Gefter, W. (1985). Stereoscopic computed three-dimensional surface display. *Radio. Graphics*. 5, (825-852).

[6] Ponmary P., & Jeya S. (2009). A dynamic 3D clustering algorithm for the ligand binding disease causing targets. *IJCSNS International Journal of Computer Science and Network Security*. 9, 274-276.

[7] Ashburner, J., & Friston K. (2003). Image segmentation.

[8] Felazenszwalb, P., & Huttenlocher D. (2004). Efficient Graph-Based Image Segmentation. *International Journal of Computer vision.* 59, 167-181.

[9] Miguel, S., Lambert, R., Miguel, C., Jorge, J., Amparo, M., Pablo, G., Tahoces, J., Martin, C., & Pierre C. (2013). Quantification of Right and Left Ventricular Function in Cardiac MR Imaging & Comparison of Semiautomatic and Manual Segmentation Algorithms" *Diagnostics*, 2075-4418.

[10] Senthilkumaran, N., & Rajesh, R. (2009). A Study on Edge Detection Methods for Image Segmentation. *Proceedings of the International Conference on Mathematics and Computer Science*, 255-259.

[11] Lakshmi, S., & Sankaranarayanan, V. (2010). A study of Edge Detection Techniques for Segmentation Computing Approaches. *IJCA Special Issue on "Computer Aided Soft Computing Techniques for Imaging and Biomedical Applications"* 13-25.

[12] Senthilkumaran, N., & Rajesh, R. (2008). A Study on Split and Merge for Region based Image Segmentation, *Proceedings of UGC Sponsored National Conference Network Security* (NCNS-08). 57-61.

[13] Senthilkumaran, N., & Rajesh, R. (2009). Edge Detection Techniques for Image Segmentation – A Survey of Soft Computing Approaches. *International Journal of Recent Trends in Engineering*. 1, 250–254.

[14] Abdullah A., & Dia M. (2014). Packet Features Extractor for Network Security Systems: Design and Implementation, *International Journal of Engineering and Innovative Technology (IJEIT)*. 3, 10.

[15] Xiaohan, Y., & Yla-Jaaski, J. (1992). Image Segmentation Combining Region Frowing and Edge Detection. *Image,Speech and Signal Analysis,Proceedings,11th IAPR International Conference*. 481-484.

[16] Lee, Y., Song, S., Lee, J., & Kim, M. (2005). Tumor Segmentation from Small Animal PET using Region Frowing Based on Gradient Magnitude. *Enterprise networking and Computing in Healthcare Industry, HEALTHCOM. Proceedings of 7th International Workshop on*. 243-247.

[17] Kannan, R. (2008). A new Segmentation System for Brain MR Images Based on Fuzzy Techniques, *Applied Soft Computing for Dynamic Data Mining*. 8, 4, 1599-1606,

[18] He, SJ., Wng, X., Yang, Y., & Yan, W. (2000). MRI Brain Images Segmentation. *Circuit and System 2000, The 2000 IEEE Asia-Pacific Conferance*. 113 – 116.

[19] Rajini, N., & Bhavani, R. (2011). Enhancing K-means and Kernelized Fuzzy C-Means Clustering with Cluster Center Initialization in Segmenting MRI Brain Images. *Electronic Computer Technology (ICECT),2011 3rd International Conference*. 259 – 263.

[20] Hoi, CH., H., & Lyu, M., R. (2004). Novel log based relevance feedback technique in content based image retrival. *Proceedings of thhe12th annual ACM international conference on Multimedia*. 24-31.

[21] Zhung, XS., & Huang, TS. (2003). Relevance Feedback in Image Retrival: A Comprehensive Review. 8, 6, 536-544,.

[22] Zhang, Q., Goldman, SA., Yu, W., & Fritts, JE. (2002). Content Based Image Retrival using Multiple Instance Learning. *19th International Conf. on Machine Learning*. 682-689.

[23] Arbelaez, P., Maire, M., & Fowalkes, C. (2011). Contour Detection and Hierarchical Image Segmentation. *Pattern Analysis and Machine Intelligence, IEEE Transactions.* 33, 898-916.

[24] Malczewski, K., & Stasinski, R. (2008). Toeplitz-Based Iterative Image Fusion Scheme for MRI. *in Proceedings of the IEEE International Conference on Image Processing*. 341–344.

[25] Ibrahiem, M., & Emary, E. (2006). On the Application of Artificial Neural Networks in Analyzing and Classifying the Human Chromosomes, *Journal of Computer Science*. 2, 72-75.

[26] Isa, N., Salamah, S., & Ngah, U. (2009)Adaptive Fuzzy Moving K-Means Clustring Algorithm for Image Segmentation. *Consumer Electronics,IEEE Tansactions*, 55, 4, 2145-2153.

[27] Rajini N., & Bhavani, R. (2011). Enhancing K-means and Kernelized Fuzzy C-Means Clustering with Cluster Center Initialization in Segmenting MRI Brain

Images. *Electronic Computer Technology (ICECT),2011 3rd International Conference*. 259 – 263.

[28] Zhang, Q., Goldman, S., Yu, W., & Fritts J. (2002) Content Based Image Retrival using Multiple Instance Learning. 682-689.

[29] Li, W., Yong, Z., & Shixiong, X. (2007). A Novel Clustering Algorithm Based on Hierarchical and K-Means Clustering," *Control Conference, 2007, Chinese*. 605-609.

[30] Bezdek, JC., Ethrlich, R., & Full, W. (1984). FCM: The Fuzzy c-Means Clustering Algorithm. *Computers & Geoscience.* 10, 191-203,.

[31] Abdullah A., & Dia M. (2014). Packet Features Extractor for Network Security Systems: Design and Implementation, *International Journal of Engineering and Innovative Technology (IJEIT).* 3, 10, 1166-1169.

[32] Bezdek, JC., Hall, LO., & Clarke, L. (1993). Review of Image Segmentation Techniques using Pattern Recognition. *Medical Physics*, 20, 14, 1033-1048.

[33] Steger, C. (1998). An unbiased detector of curvilinear structures. *IEEE Transactions on Pattern Analysis and Machine Intelligence*, 20, 113–125.

[34] Neoh, H., & Hazanchuk, A. (2004). Adaptive Edge Detection for Real-time Video Processing using FPGAs. *Global Signal Processing*. 978-996.

[35] Zhou, X., Zhang, CH., & Li, S. (2006). A preceptive uniform pseudo-color coding method of SAR images. *IEEE Transactions.* 6, 1-2.

[36] Jung, H., & Wu, N. (2010). MRI Brain Image Detection Based on Color-Converted K-Means Clustering Segmentation. *Measurement,* 43, 7, 941-949.

[37] Clark, K., Vendt, B., Smith, K., Freymann, J., Kirby, J., Koppel, P., Moore, S., Phillips, S., Maffitt, D., Pringle, M., Tarbox, L., & Prior, F. (2013). The Cancer Imaging Archive (TCIA): Maintaining and Operating a Public Information Repository, *Journal of Digital Imaging*. 26, 6, 1045-1057.

[38] Keith, A,. & Johnson, M. (1995-1999). Tissue Signal Characteristics. *Harvard Medical School.*

[39] Pereira, M. (2010). Biomedical Diagnostic and Clinical Technologies Apply High-Performance Cluster and Grid Computing,

[40] Andrea S., Guido P., & Heinz-Otto P. (2000). Efficient Semiautomatic Segmentation of 3D Objects in Medical Images. *MeVis – Center for Medical Diagnostic Systems and VisualizationUniversitaetsallee 29, 28359 Bremen, Germany*. 1935.

[41] Uma, G., Vetri, S., & Nadarajan, R. (2010). DICOM Image compression using Bilinear Interpolation. *Information Technology and Applications in Biomedicine (ITAB), 2010 10th IEEE International Conference*. 1 – 4.

[42] Ponmary, P., & Jeya, S. (2009). A dynamic 3D clustering algorithm for the ligand binding disease causing targets. *IJCSNS International Journal of Computer Science and Network Security*. 9, 274-276.

[43] Gobert, N., & Hiroshi F. (2007). K-means Clustering for Classifying Unlabelled MRI Data. *Proceedings of the 9th Biennial Conference of the Australian Pattern Recognition Society on Digital Image Computing Techniques and Applications.* 92-98.

[44] Dubey, R., B., Hanmandlu, M., & Gupta, K. (2010). An advanced technique for volumetric analysis. *International Journal of Computer Applications*. 1, 1, 91-98.

[45] Hossam, M., Moftah, A., & Mohamoud S. (2010). 3D Brain Tumor Segmentation Scheme using K-mean Clustering and Connected Component Labeling Algorithms. *2010 10th International Conference on Intelligent Systems Design and Applications*. 320 - 324.

[46] Jovisa, Z., Kaoru, H., & Carlos, M. (2008). Compactness Measure for 3D Shapes. *IEEE/OSAIIAPR International Conference on Informatics, Electronics & Vision,* 41, 2, 1180 - 1184.

[47] Gonzalez, C., & Woods, E. (2002). Thresholding. In Digital Image Processing. *Pearson Education*. 595–611.

[48] Tokuzo, K., Kiichiro, S., Toru, K., Yoshiaki, O., & Toshio, S. (1971). Circularity Ratio- Certain Quantitative Expression for the Circularity of a Round Figure. *Okajimas Fol. anat. Jap*. 48, 153-162.

[49] Akmal, R., Nur, Z., Abdul-lah, B., Mohd, S., & Ismail, M. (2010). Connected component labeling using components neighbors-scan labeling approach. *Journal of Computer Science*. 6, 10, 1070-1078.

[50] Alan, W., & Addison W. (2000). 3D Computer Graphics (3rd edition).

[51] Micheal, B., KarlHeinz, H., Ulf, T., & Martin, R. (1990). 3-D Segmentation of MR Images of the Head for 3D Display. *IEEE Transaction on Medical Imaging*. 9, 2, 83-177.

[52] Leif, K., Mark, P., & Pierre, A. (2010). Polygon Mesh Processing.

[53] Rahnamayan, S., & Mohamad, S. (2010). Tissue Segmentation in Medical Image Based on Image Processing Chain Optimization. *International Workshop on Real Time Measurement, Instrumentation & Control [RTMIC]*. 18, 2, 107-112.

[54] Mikulka, J., Burget, R., Riha, K., & Gescheidtova, E. (2013). Segmentation of brain tumor parts in magnetic resonance images. *2013 36th International Conference of Telecommunications and Signal Processing (TSP).* 565 – 568.

[55] Hore, A., & Ziou, D. (2010). Image Quality metrics: PSNR vs. SSIM," *Pattern Recognition (ICPR), 2010 20th International Conference*. 2366-2369.

[56] Zhang, N., Ruan, Su,. Stéphane, L., Qingmin, L., & Yuemin, Z. (2010). Kernel feature selection to fuse multi-spectral MRI images for brain tumor segmentation *Computer Vision and Image Understanding. 2010 Elsevier*. 115, 2, 256-269.

[57] Li, X., Lebonvallet, S., Qiu, T., & Ruan, S. (2007). An improved level set method for automatically volume measure: application in tumor tracking from MRI image. *29th Annu. Int. Conf. Engineering in Medicine and Biology Society (EMBS'07)*. 808–811.

[58] Magdi, B., Amien, M., Ahmed, A., & Walla, I. (2013). An Intelligent-Model for Automatic Brain-Tumor Diagnosis based-on MRI Images. *International Journal of Computer Applications.* 72, 23, 20-24.

[59] Jan, M., Radim, B., Kamil, I., & Eva, G. (2013). Segmentation of Brain Tumor Parts in Magnetic Resonance Images. *2013 36th IEEE International* Conference *on Telecommunications and Signal Processing (TSP).* 565 – 568.

[60] Ruan, S., Lebonvallet, S., Merabet, A., & Constans, J. (2007). Tumor segmentation from a multi-spectral MRI images by using support vector machine classification. *4th IEEE Int. Symp. Biomedical Imaging*. 1236–1239.

[61] Chang, H., & Robes, U. (2000). Face detection.

[62] Lindeberg (2013). Image Matching Using Generalized Scale-Space Interest Points. *Scale Space and Variational Methods in Computer Vision, Springer Lecture Notes in Computer Science.* 7893, 355-367.

[63] Chaddad, A., Zinn, P.O., & Colen, R. (2014). Quantitative texture analysis for Glioblastoma phenotypes discrimination. *Control, Decision and Information Technologies (CoDIT), 2014 International Conference*. 605 – 608.

[64] Ernesto, B. (2007). An easy measure of compactness for 2D and 3D shapes. *2007 Pattern Recognition Society. Published by Elsevier Ltd*. 41, 1275–1284.

[65] Jovisa, Z., Kaoru, H., & Carlos, M. (2012). Compactness Measure for 3D Shapes. *IEEE/OSAIIAPR International Conference on Informatics, Electronics & Vision*. 40, 1180 - 1184.

[66] Ballard, H., & Brown, M. (1982). Computer Vision, *Prentice-Hall, EnglewoodCliffs, NJ*.